GEORGE C. MARSHALL SPACE FLIGHT CENTER

HUNTSVILLE, ALABAMA

[redacted]

WELDING PROGRESS SUMMARY

Work Sponsored By

GPO PRICE $ ____

CFSTI PRICE(S) $ ____

Hard copy (HC) $3.00

Microfiche (MF) $ .75

ff 653 July 65

Welding Development Branch
Ianufacturing Engineering Laboratory
orge C. Marshall Space Flight Center

Prepared For And Distributed By

Technology Utilization Office
George C. Marshall Space Flight Center

FACILITY FORM 602

N66 21784 (ACCESSION NUMBER)	(THRU)
87 (PAGES)	1 (CODE)
TMX 57330 (NASA CR OR TMX OR AD NUMBER)	15 (CATEGORY)

National Aeronautics and Space Administration

NASA

Rgt 33715

MSFC - Form 454 (Revised September 1961)

SUMMARY

QUANTITATIVE ANALYSIS OF TIME TEMPERATURE EFFECTS IN 2219 ALUMINUM WELDING

Conference February 18, 1965
MSFC - R-ME
Huntsville, Alabama

ABSTRACT

QUANTITATIVE ANALYSIS OF TIME TEMPERATURE
EFFECTS IN 2219 ALUMINUM WELDING

I. Introduction:

The welding process as applied to metals joining is often referred to as the "art" of welding rather than the "science" of welding. To place welding on a scientific level, in a space age environment that demands better strength to weight ratios, we must utilize quantitative data analysis tools such as experimental design, regression anaylsis and other related mathematical tools.

The quantitative data analysis approach is used in this study to determine which controllable effect the time-temperature relationship in welding 2219 Aluminum Alloy. By controling these time-temperature relationships, weld variable responses can be predicted, controlled and ultimately optimized.

II. Expressions for Heat Input:

A. Joules/In/In

For many years, Joules/In/In has been used for an expression of heat energy input. This expression is used in various welding publications today. This expression is not adequate for expressing weld heat input since various combinations of the independent variables voltage, current and travel speed will give the same expression for Joules/In/In but gives quite different responses.

B. Time Temperature

The time-temperature characteristic curve is felt to provide an adequate expression for weld heat input. Maximum temperature is defined as the peak temperature the material reaches during the welding cycle. Time@ temperature is defined as the time that the material being welded is above that temperature that adversely affects strength properties of the base material.

III. Approach:

There is a particular "set" of time-temperature characteristics curves that optimize such weld variable responses, as weld strength properties. The "set" of curves for this investigation are those taken from temperature measurements in the weld bead, $\frac{1}{4}$", $\frac{1}{2}$", 1" and 2" from the center of the weld bead.

To control and reproduce such time-temperature curves, we must define and establish quantative relations between maximum temperature, time-at-temperature and their independent variables. Once these relationships have been established, the time-temperature characteristic curve can be reproduced within tolerances, based on the confidence level of the curves.

With the ability to control and reproduce the time-temperature characteristics curve within acceptable tolerances one will be in a position to predict and optimize weld variable responses.

To define the time-temperature functional and response relationships it was necessary to establish the following basic mathematical relationships:

$$Y_1 = F(X_1, X_2)$$
$$Y_2 = F(X_1, X_2)$$
$$Y_3 = F(X_1, X_2)$$

and

$$X_1 = F(X_3, X_4 \ldots X_9)$$
$$X_2 = F(X_3, X_4 \ldots X_9)$$

where:

Y_1= Yield strength
Y_2 = ultimate strength
Y_3 = elongation
X_1 = maximum temperature
X_2 = time @ temperature
X_3 = voltage
X_4 = current
X_5 = travel speed
X_6 = wire speed
X_7 = torch angle
X_8 = gas flow
X_9 = tungsten length

A fractional factorial experimental design was used with the range of each independent variable set at predetermined high and low points. Four replications were conducted at the midpoint of the range to aid in the development of regression equations.

The critical independent and dependent variables were recorded with the aid of low speed tachometers, thermocouples and other measurement devices.

A step-wise multiple regression analysis was used to develop mathematical relationships between the controllable independent variables. A quadratic equation solution program was utilized to solve the regression equations based on pre-determined increments of the independent variables.

IV. Result: Maximum Temperature @ Time @ Temperature

The results of this study indicates something contrary to our belief prior to this investigation, that is; time @ temperature does not play as significant a role in determining strength properties as believed. I say this with some qualification, at lower maximum temperature an increase time @ temperature above approximately 24 seconds did not contribute to a decrease in ultimate strength, however at maximum temperatures above approximately 1250°F an increase in time @ temperature caused a decrease in strength properties throughout the time @ temperature range investigated.

Based on the results it was found that a maximum yield and ultimate strength of 35,128 psi and 54,388 psi respectively could be obtained with a maximum temperature of 1500°F/& a time temperature of 15 seconds. The actual observed time @ temperature corresponding to the 1500°F level is approximately 52 seconds. Consequently the maximum temperature observed corresponding to a time @ temperature of 16 seconds was approximately 860°F. From a practical view point it would appear difficult to attain these valves of 1500°F for maximum temperature and 16 seconds for time at temperature unless some exotic chilling mechanism could be developed. If it is practical to reproduce these values that optimize strength properties, this fast cooling rate could have an adverse effect on the overall weld properties by increasing crack formation.

For elongation we had a different situation as far as values that produced acceptable elongation properties. A value of 4.87% elongation was obtained with a maximum temperature of 1500°F and a time @ temperature of 52 seconds. In seeking to optimize elongation properties we go to the opposite end of the time @ temperature scale for a value of 52 seconds. The value for elongation obtainable when we optimize yield and ultimate strength was 4.38%.

Controllable Weld Variables vs Max. Temperature and Time @ Temperature

In analyzing the controllable weld variables, there are four variables that contribute significantly to variation in strength properties. They are:

Voltage
current
travel speed
wire speed

and we will call them primary weld variable. This is not to infre that variables such as gas flow aee not important only that a variation in this variables does not contribute significantly to a variation in the strength properties of the weldment.

There was not a combination of controllable weld variables that gave values of time @ temperature and maximum temperature in a combination of 16 seconds and 1500°F respectively.

The combination of controllable weld variables that come nearer giving the value of time @ temperature and maximum temperature was:

voltage - 10.4 volts
current - 185 amps
travel speed - 6.0 in/min
wire speed - 19.4 in/min
torch angle - 1/2° lead
gas flow - 120 CFH
tungsten length - .38 in

These values for time @ temperature and maximum temperature are:

time @ temperature - 29.0 sec
maximum temperature - 14,685°F

The corresponding strength property values are:

yield strength - 30,691 psi
ultimate strength - 40,165 psi
elongation - 2.89

<u>Conclusions</u>:

To date, based on observed data, it is felt the time-temperature approved to controlling weld variables is feasible. Temperature measurements other than in the weld bead alone should be relied upon for a three dimensional temperature profile.

In addition, it is felt that the time-temperature characteristics curves can be shaped to produce increased strength properties. This can be accomplished by utilizing improved independent variable control techniques and chilling mechanisms. However, the limits of time-temperature approach will have to be defined taking into consideration the effects on defect levels such as weld cracking and porosity formation characteristics.

SUMMARY PROGRESS REPORT

on

WELDING BASE METAL INVESTIGATION

to

GEORGE C. MARSHALL SPACE FLIGHT CENTER
NATIONAL AERONAUTICS AND SPACE ADMINISTRATION

from

BATTELLE MEMORIAL INSTITUTE

February 24, 1965

OBJECTIVE

The objective of this research is to study the effects of base metal and filler metal chemical content, gas content, internal impurities, and external impurities upon the occurrence of weld defects in the aluminum alloys 2219 and 2014.

PROGRAM APPROACH

The research in this program is divided into two phases. In Phase I, the effects of the above factors are studied using bead-on-plate welds with no filler metal added. In Phase II, the effects of the above factors are studied using controlled-composition filler metals to deposit bead-on-plate welds.

Four steps were used in the program. First, materials were prepared with controlled levels of four factors: chemical content, gas content, internal impurities, and external impurities. Second, welds were made in these materials under carefully controlled conditions. Third, the welds were examined visually and by radiographic and metallographic methods to determine the type, number, and size of weld defects present. Finally, the results were analyzed to determine the effects of the four factors. The program was statistically planned and the results are being analyzed statistically. All welding equipment and instrumentation are accurate to specified requirements so that the data obtained in this program will be transferable to other programs.

DEFINITIONS

The chemical content of the base plate in this program is defined as those metallic elements for which both a maximum and a minimum level is specified in current alloy specifications (Cu, Mn, V, Ti, and Zr for 2219 base plate and Cu, Mn, Si, and Mg for 2014). Gas content is defined as the hydrogen in the metal which is detected by vacuum-fusion analysis. Internal impurities are defined as those elements for which only a maximum level is specified (primarily Si, Fe, Mg, and Zn in 2219 base plate and Fe, Zn, Ti, and Cr in 2014). External impurities are defined as the purity of the helium shielding gas used during the welding. The low external impurity atmosphere has a -60 F dewpoint. The high external impurity atmosphere has a +10 F dewpoint. The base plate used in both atmospheres is chemically cleaned prior to welding.

MATERIALS

Two levels of each factor were studied. Eight different material "types" were fabricated. Each type contained a different combination of levels of the four factors. The level of each factor for each type is shown in Table 1. As shown in Table 1, the hydrogen content of the finished plate was not completely controlled by any of the methods described in Table 2. The three other factors, chemical content, internal impurities, and external impurities were controlled successfully.

The hydrogen content of an available lot of commercial 2219 base plate was about 0.1 ppm by weight. No commercial 2014 base plate was available for analysis.

WELDING

All test welds made during Phase I were deposited in the horizontal position as bead-on-plate welds with no filler metal. All welds were made with the d-c straight polarity TIG process utilizing an automatic, voltage-regulating head. Arc amperage, arc voltage, and arc travel speed were carefully regulated and precisely recorded for each weld. Welding was conducted in a vacuum-purged controlled-atmosphere chamber to insure reproducible gas-shielding conditions.

DEFECT STUDY

Pores were the only significant weld defects observed during Phase I. Most of the pores were so fine that they were not visible in radiographs of the welds. A point counting method was used to determine the porosity level of

TABLE 1. COMPOSITIONS OF X2014[a] AND X2219[a] BASE PLATE

Type Number	Chemical Content[b]	Internal Impurities[b]	External Impurities[b]	Target H_2 Content[b]	Actual H_2 Content X2219 1/4 in.	Actual H_2 Content X2219 3/4 in.	Actual H_2 Content X2014 1/4 in.	Actual H_2 Content X2014 3/4 in.
1	L	L	L	L	.1	.3	.3	.3
2	L	H	L	H	.8	.5	.7	1.9
3	L	H	H	L	.6	.5	.4	.7
4	L	L	H	H	.3	.1	.4	1.8
5	H	L	L	H	1.1	.7	.6	.5
6	H	H	L	L	.5	.4	.8	.7
7	H	L	H	L	.1	.1	.5	.3
8	H	H	H	H	.7	.5	.9	.8

(a) The prefix "X" denotes materials prepared in the laboratory to distinguish them from commercial materials.

(b) L = Low Level.
H = High Level.

TABLE 2. CONTROL OF HYDROGEN CONTENT

I. Low Hydrogen Content (target of less than 0.2 parts per million by weight of hydrogen)

Method 1: long chlorination time (15 minutes)

low pouring temperature (1300 F)

(X2319-1, 3, 6, 7; X2219-1, 3, 6, 7; X2014 only 1/4 inch type 3 plate)

Method 2: no chlorination

long holding time (20-30 minutes)

low pouring temperature (1300 F)

(X2014-1, 3, 6, 7 only 3/4 inch type 3 plate)

II. High Hydrogen Content (target of more than 1.0 ppm hydrogen by weight)

Method 1: short chlorination time (6 minutes)

long holding time at high temperature (25 minutes at 1500 F)

(X2319-2, 4, 5, 8; X2219-2, 8)

Method 2: no chlorination

gas flame played over melt with mild stirring (5-10 minutes, metal at 1400-1450 F)

(X2219-4, 5; X2014-2, 5, 8)

Method 3: melt stirred with graphite rod wet with water at frequent intervals

(X2014-4)

from two to four metallographic cross sections taken from each weld. The cross sections were photographed at 20X and a grid of at least 10 lines per inch was superimposed on the final print during the photographic processing. A typical weld cross section with a superimposed grid is shown in Figure 1. Two quantities were obtained from each photograph. The total number of grid intersections within the weld fusion zone was obtained by measuring the fusion zone area with a planimeter and multiplying this by the number of grid intersections per unit area. The number of grid intersections that coincided with pores in the weld was obtained by counting. The per cent porosity is equal to the number of intersections coincident with pores divided by the total number of intersections within the weld, times 100. Table 3 lists the average porosity level for each type of base plate composition (see Table 1 for the composition of each type).

Segregation and Porosity Occurrence

During the study of a limited number of cross sections of welds, a relationship was noted between segregation in the weld and the occurrence of pores in the weld. Figure 2 shows a transverse section of a weld made on X2219 base plate. A microhardness traverse across the weld revealed a hardness difference between the light bands in the weld (in which most of the pores were located) and the dark bands. The hardness traverse gave no conclusive results above Point 6, in Figure 2, where the resolution of the bands was difficult.

Figure 3 is a photomacrograph of a longitudinal section of a weld on X2014 base plate. The pores were observed to be ordered by size and were distributed in families of curves. A study of a limited number of other longitudinal weld sections, both porous and nonporous, showed several common features. The welds all contained two distinct domains of pore or segregation grouping: one in the lower part of the weld and one in the upper part. The similar features of shape and size of porous areas and of segregated areas within the weld related occurrence of pores to weld solidification on a microscopic scale. Further study of pore occurrence will be made in later work during this program.

OBSERVATIONS AND CONCLUSIONS

The following observations and conclusions were made tentatively since the analysis of results is not complete:

(1) Tentatively, the significance of the high levels of the four factors can be ranked according to their effect on the porosity level. A high level of external impurities caused the porosity level to be significantly higher than the porosity level caused by a high level of gas content or internal impurities. A high chemical content was the least significant and caused the lowest porosity levels.

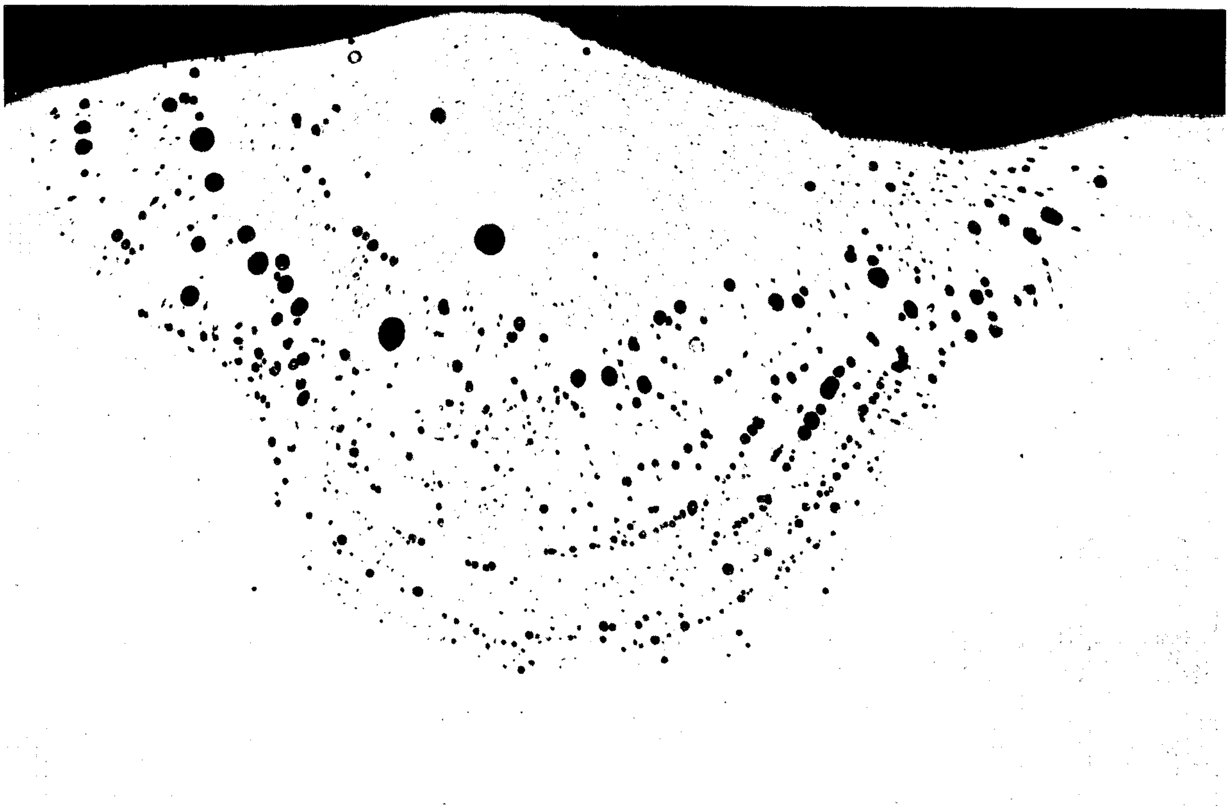

20X Etch-Polish RM40008

FIGURE 1. TYPICAL CROSS SECTION OF 3/4-INCH-THICK X2219-8 WELD
GW-87 cross section 10 inches from end of weld.
Porosity = 11.0%.

TABLE 3. AVERAGE POROSITY LEVELS FOR WELDS IN X2219 AND X2014 BASE PLATE

	Average Porosity Level, per cent			
	X2219 base plate		X2014 base plate	
Type Number	1/4 inch thick	3/4 inch thick	1/4 inch thick	3/4 inch thick
1	0	0	0	0
2	0	0	0	0
3	4.9	6.0	9.6	14.2
4	4.0	4.3	4.9	19.7
5	0	0	3.1	0
6	0	0	3.0	0
7	3.7	3.9	6.1	13.5
8	7.2	10.2	11.1	15.3

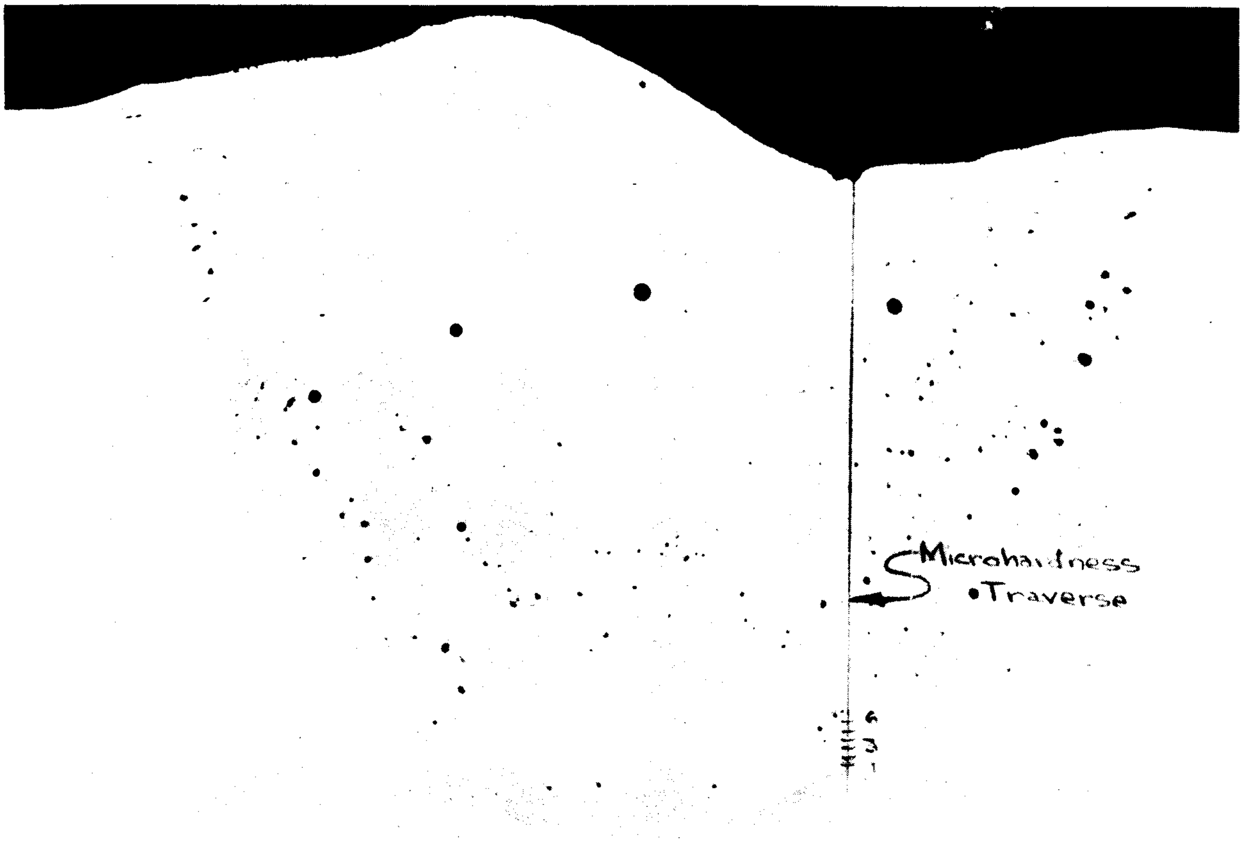

20X Etch-Polish RM40635

FIGURE 2. LOCATION OF MICRO-HARDNESS VARIATIONS IN X2219 WELD

Point*	Hardness Knoop hardness number**	Band
1	83.0	Dark
2	83.0	Dark
3	73.5	Light
4	71.5	Light
5	80.5	Dark
6	77.0	Dark

* Results above Point 6 not reported due to interpretation difficulties.

** 50-gram load.

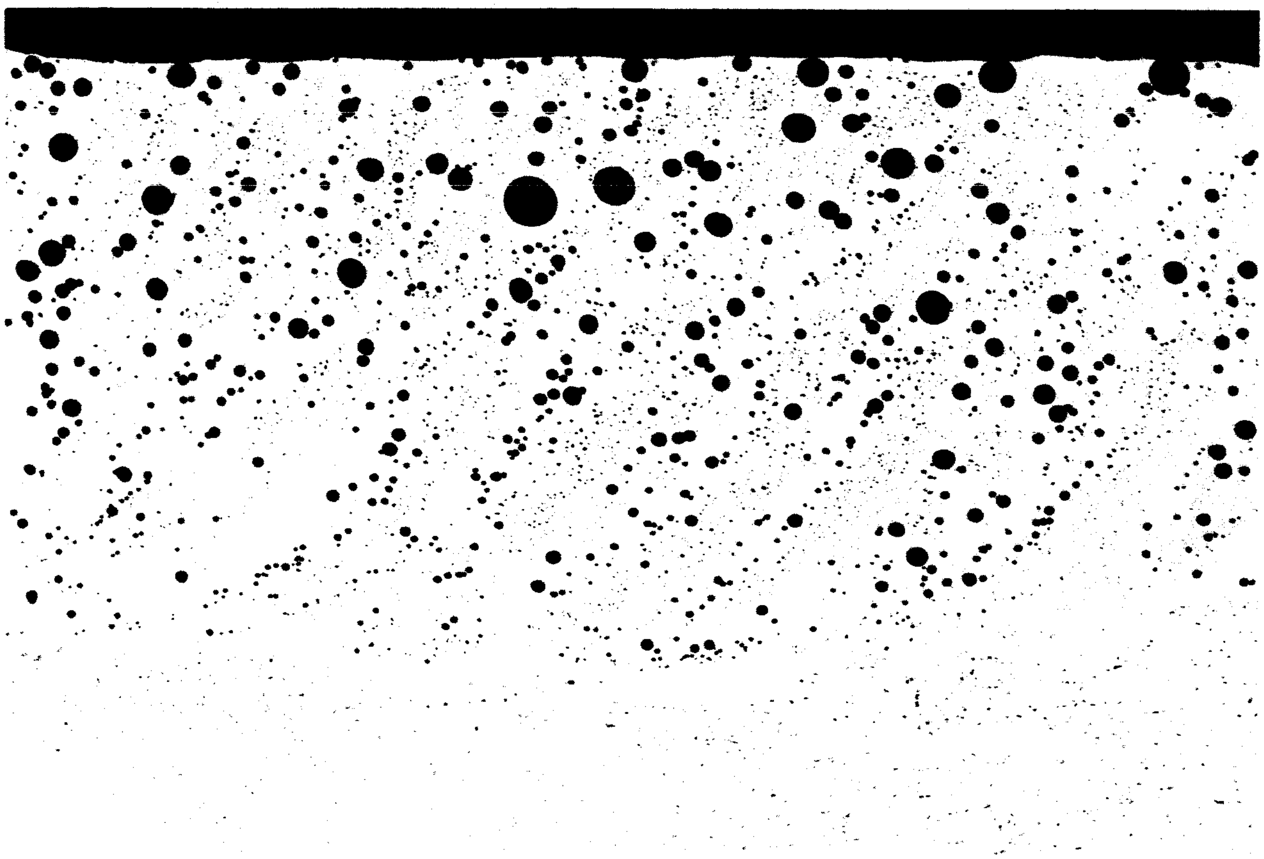

20X 5% HF RM41859

FIGURE 3. PREFERENTIAL PORE OCCURRENCE IN A WELD ON X2014-4 BASE PLATE

(2) An interaction between internal impurities and chemical content which affected the weld porosity level was conclusively demonstrated for 3/4-inch-thick X2219 base plate. With a low internal impurity level, the porosity level did not change significantly when the chemical content was changed from low to high (gas content and external impurities remained constant). With a high internal impurity level, the porosity level doubled when the chemical content was changed from low to high (gas content and external impurities remained constant).

(3) The higher porosity levels in X2014 base plate welded in a helium atmosphere of about +10 F dewpoint indicated that X2014 welds were more sensitive to moisture in the shielding gas than were X2219 welds.

(4) Pores were observed to occur in welds made in low dewpoint shielding gas only on 1/4-inch-thick Types 5 and 6 compositions of X2014 base plate (see Table 1).

(5) Some fabrication problems were encountered with base plates of 1/4-inch-thick X2014 and X2219 Types 5 and 7 compositions. Some plates of these types contained minute surface cracks not detectable by ultrasonic inspection to Class "A" of MSFC-SPEC-283.

FUTURE WORK

Work planned for the completion of the program is summarized below:

(1) The analysis of welds made on base plate with no filler wire will be completed.

(2) Eight separate compositions of X4043 and X2319 filler wire will be used to deposit bead-on-plate welds on 2014 and 2219 base plate, respectively.

(3) Defects in the welds made with filler wire will be studied and the results will be analyzed.

PROGRESS REPORT

ON

STUDY OF THE MECHANISMS OF POROSITY FORMATION IN WELDS

CONTRACT NAS 8-11332

PRESENTED TO

WELD JOINT PERFORMANCE IMPROVEMENT COMMITTEE

MARSHALL SPACE FLIGHT CENTER

February 18, 1965

BY

D. D. POLLOCK

DOUGLAS AIRCRAFT CO., INC.
SANTA MONICA, CALIFORNIA

ABSTRACT

A theoretical model for the formation of porosity in aluminum welds is presented in terms of nucleation and growth theory. The limitations of both the theory and the techniques are discussed.

Since limited data are available, only tentative trends can be observed. A good correlation appears to exist between the microscopic and specific gravity measurements for volume fraction of porosity. The total hydrogen content of weld pools, pore nucleation and pore growth all appear to show consistent behavior. Initially, the porosity nucleates as many fine pores. With increasing weld solidification times the pores grow and have time to escape from the melt. Other smaller pores which form during and after this agglomeration phase have time for some growth, but not enough time to leave the weld. This is evidenced by decreases in the total hydrogen contents and in the pore growth rates and a small increase in the pore nucleation rates which occur after maximum escape of hydrogen from the weld pool. The reasonable agreement of the pore volume fraction as a function of the Johnson-Mehl parameter gives confidence that the theoretical and practical approximations and the resultant data are reasonably well founded.

Future work is outlined.

INTRODUCTION

This work represents an attempt to explain the mechanisms responsible for porosity in aluminum welds in terms of metallurgical phenomena as well as welding parameters. Hydrogen is considered to be largely responsible for this problem. The kinetics of this behavior are not well known. Thus, the major emphasis is being placed upon the way in which porosity forms and grows.

THEORETICAL BACKGROUND

Consider a molten metal, or alloy, of a given initial composition which is exposed to a gas under equilibrium conditions. This assumes that the temperature of the liquid-gas system and the composition and pressure of the gas will remain constant. The composition of the gas is considered to be constant because the vapor pressure of most liquid metals is small near the melting point. Under these conditions, some of the gas will be absorbed by the liquid metal. The amount of such absorption is a function of the partial pressure of the gas. Another way of expressing this is: the amount of gas absorbed by the liquid metal will depend upon the quantity of that gas in contact with the liquid metal. This will be a constant for any given set of "equilibrium" conditions.

If the equilibrium conditions change, the amount of gas dissolved by the liquid will change. If the composition and pressure of the gas are held constant and the temperature is increased, the amount of dissolved gas will usually increase. If the temperature is decreased, the quantity of dissolved gas will also decrease. Thus, for most liquid metals, as the temperature of the melt decreases, the amount of gas which the liquid can contain in solution decreases sharply. That portion of the gas which the liquid metal cannot retain is

rejected from the melt as the familiar porosity seen in castings and welds.

The question is how does such rejection of gas from the melt occur? The most convenient way of understanding this behavior is based upon thermodynamics and provides a probability of whether or not the reaction will occur. The thermodynamic measure of this behavior is called the change in free energy of the system (ΔF). It, however, does not provide information as to the rate of the reaction.

Under the equilibrium conditions previously noted, the quantity of gas in solution in the liquid metal was constant; in this case $\Delta F = 0$ and no change will occur. When the temperature of the melt is decreased, ΔF will be negative and a decrease in the solubility of the gas is expected. Conversely, when the melt temperature is raised, no gas rejection will occur; actually, more gas will be dissolved. Under these conditions, ΔF will be positive. Thus, the sign of ΔF indicates whether a reaction will or will not occur.

In order to employ this concept for evaluating porosity formation something must be known about the behavior of a molten liquid which contains gas atoms in solution. A convenient picture of this consists of an assembly of metal and some gas atoms, which are in rapid, random motion. In this state several gas atoms will occasionally encounter each other. They may remain together, or they may separate. If the conditions are proper, they remain together and little clusters of gas atoms will persist and grow in the melt. These are known as gas nuclei and are assumed to be tiny spheres. Changes in the pressure and composition of the gas and the temperature of the melt can cause these nuclei to grow or to disperse.

For a given set of conditions the formation or dissolution of nuclei can be predicted by the sign of ΔF. The temperature, pressure and composition of the gas over the melt and an approximation of the smallest size of a stable nucleus must be considered for this prediction. When the other variables are maintained at a constant level, the size of the smallest stable nuclei can be used to predict the sign of ΔF.

This approach readily provides an approximation for ΔF; ΔF is found to vary inversely as the square of the radius of the nucleus. This information permits an approximation of the nucleation rate. This is also found to vary inversely as the square of the radius of the nucleating particle. Unfortunately, the radius of the nucleus cannot be measured directly during the welding cycle.

One way of circumventing this problem is to utilize the time-temperature cycle that the weld undergoes during solidification. This will provide a measure of nucleus size.

Since the aluminum alloys under consideration here are representative of eutectic systems (which show a pronounced thermal arrest upon solidification), their thermal arrests may be used as an "anchor point" upon which to base the subsequent calculations. For a given heat input per unit volume of metal and relatively constant cooling conditions, the temperature of this thermal arrest will occur at a nearly constant temperature. This fact is useful in simplifying the expressions for approximating the rate at which these nuclei form. It is also important to note that most of the porosity formation will have been completed by the time that this temperature is reached. Thus, this temperature marks the lower limit of pore formation.

Since heating and cooling rates are very fast and temperatures are difficult to measure, the time to reach the eutectic or "anchor" temperature is used to measure the time available for pore formation. This also gives a readily measurable but indirect approximation of the temperatures andcooling rates that are of interest in welding.

Now, knowing the time for a weld to reach the eutectic temperature and the relationship previously obtained for the nucleation rate, the nucleation rate is found to be approximately inversely proportional to the square of the time required to cool the weldmetal to the eutectic temperature - a more readily useable relationship than one based upon exact temperatures or nuclei sizes.

In a similar way the growth rate of the nuclei can be shown to be approximately directly proportional to the square of the time required for the weld to cool to the eutectic temperature. Other quantities such as the area fraction occupied by pores and the average pore size can also be approximated in this way. The derivations of these relationships are given in the appendix.

EXPERIMENTAL METHODS FOR DETERMINING PORE RELATIONSHIPS

The methods of obtaining pore data to verify the theory are briefly described below. The significant pore parameters are obtained by metallographic examination. Sections of a given weld nugget are examined under magnification using a grid which is about 0.04 x 0.04 inches and contains 144 squares. The pores in each grid are counted and an estimate of their area is made. This process is continued until the entire section has been explored. The average pore area is obtained by adding all of the pore areas and dividing this quantity by the total number of pores. The average pore area permits the calculation of the average pore radius. The volume of the average pore

divided by the time to reach the eutectic temperature provides an approximation of the average pore growth rate. The total number of pores divided by the time to reach the eutectic temperature provides an approximation of the nucleation rate.

In order to make practical use of these relationships the way in which they were derived must be kept in mind. The precise mechanism of nuclei formation is not known on an an atomic scale and is considered to be based upon the laws of probability. Further, the theoretical relationships used in the present work are approximations. The experimental methods used for pore detection and measurement provide average values of those pores which are visible; many pores, particularly those formed just before solidification is completed, are sub-microscopic in size and cannot be included in this analysis because of the practical difficulties of counting and measuring them. In addition, the welds which are being studied here are not true welds in the sense that two pieces of metal are being joined. When these factors are considered in the light of practical applications to real welds, where many additional variables are operative, then it becomes apparent that it is imperative that the general understandings of the formation and growth of porosity be obtained. (The acquisition extremely detailed relationships would be very difficult to apply to real situations.) Thus, the primary objective of this work is to establish broad relationships regarding the factors affecting the formation of porosity which can be used to understand and minimize this problem in a practical way.

In order to establish these relationships, the variables have been selected so that they include situations encountered in welding practice. The variables to be investigated are: the contamination level of the atmosphere, the arc

current and voltage, the arc time and the material thickness. Combinations of these five factors are being tested according to a statistical plan given in Table I. This plan will permit the determination of the individual effects of the variables and will also help to indicate if any two-way interactions exist between the variables.

EXPERIMENTAL TECHNIQUES

A schematic diagram of the test apparatus is given in Figure I. Two-inch discs are being used for Phase I of the program. The specimens are cleaned with a mixture of nitric and hydrofluoric acid, rinsed in water and dried. They are then cleaned in Freon T-F vapor. The specimens are then stored in the Eringard welding box, Figure 2, where they are stored in either an atmosphere of dry helium or in a vacuum.

Prior to welding, the specimens are briefly removed from the chamber and are drilled to receive the thermocouple wires. They are again cleaned in Freon T-F vapor and returned to the chamber. The specimens are kept in the chamber overnight under a vacuum before testing. This procedure is used to minimize surface contamination, particularly moisture, which might influence the experimental results.

The specimen is placed upon the fixture, Figure 3, and the assembly is inserted into the test chamber within the Eringard welding box. A shim, Figure 4, is used to ensure that the desired distance between the top of the specimen and the electrode will be within 0.005 in. The test chamber is sealed and the controlled atmosphere is introduced into it and monitored, Figure 5, until the outlet sampling indicates that the desired atmosphere moisture content has been established. The devices which are used to measure and record welding

variables are shown in Figure 6. The prescribed welding cycle is then applied to the specimen. Upon completion of this cycle the atmosphere is again analyzed. At this point, pure dry helium is used to purge the test chamber. This is done to prevent contamination of interior of the Eringard welding box. When the purge is completed, the welded sample is removed for examination. Figure 7 shows a radiograph of a typical specimen.

After the radiograph is made, a macrophotograph of the top surface is made. The specimen is then sectioned to provide a portion of the weld which contains the center and is about 1/8"-in thick. This specimen is polished with 600 grit Al_2O_3, etched with Flick's reagent and repolished with the Al_2O_3 followed by MgO. The polished specimens are used to determine the average pore area, the average pore radius, the average growth rate and the average nucleation rate, as previously indicated. Figure 8 is a sketch of a typical pore count.

The sectioned specimen is radiographed for X-ray density measurements, Figure 9. Such measurements have not been helpful because of the very large amount of very fine porosity. These pores are too fine to permit estimates of pore fraction by X-ray techniques. After this, micrographs are made for the determination of dendrite-cell size (Figure 10). The nugget is then carefully excised with a jewellers saw and its specific gravity is measured. Following this, the nugget is chemically analyzed for hydrogen content. Selected nuggets are also given complete chemical analyses. Measurements of surface ripples have as yet not been possible to make because these do not appear on the surface of the specimens. These will be measured on the bead-on-plate specimens. The electron microscope may be of assistance in this work.

PROBLEM AREAS

Two major difficulties have been encountered. The first of these concerned the placement of the thermocouple wires. Trial runs were made on specimens to determine the size of the nuggets. When these were known, holes for the wires were drilled into the circular face so that, after welding, the thermocouple wires would be about 1/32 in. away from the nugget. This frequently resulted in the melting of the thermocouple wires. These holes are now drilled into the edge of the specimen so that their ends occupy the same locations as before. This technique almost always provides good readings. An attempt is now being made to further improve this situation by inserting a couple from one edge only. This work is not yet completed.

The second major difficulty was to select arc current-arc time combinations which would be suitable for both the 1/4-in. and 3/4-in. thick specimens. When low current-low time settings were used an extremely small weld pool resulted on the 3/4-in. specimens. When high current-high time settings were used, uncontrollable melting occurred on these specimens. This lack of control appears to have resulted from the greater volume-to-surface ratio of the thicker specimen. It was thought that the statistical plan might have to be changed. A 0.010-inch zirconia coating was applied to the specimen holder. This served to retard the heat loss from the 1/4-in. specimens without materially affecting that of the 3/4-in. specimens. This modification permitted the retention of the original statistical plan.

PRESENT STATUS OF PROGRAM

The status of the experimental work is given in Table 2. The asterisks indicate the tests which have been made or are about to be made in any given experiment. Table 3 lists the data which are now available.

The analytical data are necessarily incomplete at this time. Therefore, it is only possible to try to discern trends among the data. This is especially true since five variables are simultaneously operative. Thus, the trends discussed must be considered to be tentative; these relationships may be changed as more information is gathered.

As indicated in Figure 11, a correspondence does exist between the volume percent of porosity as determined by the microscopic and specific gravity methods. It appears that a somewhat less than ideal correlation (1.0) might be present. If this should prove to be the case, and a correlation of about 0.8 exists, useful information regarding the transfer of data from one method to the other will be available. This will also firmly establish the degree of validity of the microscopic method.

The determination of hydrogen by means of the vacuum-fusion method includes that hydrogen which was contained in the pores as well as that contained in solution in the solidified melt. Since the total hydrogen is determined, it may be impossible to separate these two contributions. However, useful information may still be obtained. It is interesting to note, Figure 12, that the total hydrogen content appears to increase for solidification times up to about 3 seconds, and decreases thereafter. It was originally considered that the hydrogen content would increase up to a given solidification time and then decrease. The decrease is considered to result from the longer opportunity for

hydrogen pores to float to the top of the melt and to escape during longer solidification times. This tendency was expected to exert a strong influence in all of this work.

The average pore nucleation rate is high for short solidification times (about 1100 pores/sec after three seconds) and decreases rapidly to about 40 pores/sec after about 5 seconds. See Figure 13. The nucleation rate then reverses its trend and begins to increase. The initial decrease in the nucleation rate is thought to result from the agglomeration of pores which have not been able to escape from the melt. A minimum amount of nucleation appears to occur at a solidification time of about 5 seconds when the agglomerated pores may have had sufficient time to escape from the molten metal. The reversal of this trend for solidification times greater than five seconds might represent the formation of "second generation" porosity which procedes as time increases but which cannot escape.

This hypothesis appears to be confirmed by the data in Figure 14. The growth rate, G, of the pores seems to reach a maximum size after a solidification time of about 3 to 5 seconds. This is presumed to represent the agglomeration phase previously noted. At solidification times of about 5 seconds maximum pore escape has apparently occurred. For longer solidification rates, the data probably represent the growth of the "second generation" of porosity which occurs after most of the original pores have left the melt. The longer solidification times permit more hydrogen to escape. The remaining pores have not had much time either to grow or to escape. This gives rise to the decreasing apparent pore growth rate.

The average pore nucleation rate changes more markedly than does the growth rate. In addition, G is very much smaller than is N. Since the pore size is

a function of G/N, the average pore size must be very small. This explains the large amount of very fine porosity which obscured the X-ray readings and precluded measurements of the pore area fraction by this means.

The pore volume fraction is shown as a linear function of the Johnson-Mehl parameter (Reference 1) in Figure 15. This is significant because the factors N and G, which previously were considered only individually as functions of time, are now combined in a complex way with time to provide a broader picture of porosity behavior. It should be noted that this function appears to be consistent over four orders of magnitude of the parameter. This lends confidence that the theoretical and practical approximations as well as the resultant data appear to be reasonably well founded.

SUMMARY

The following preliminary trends have been observed:

1. A reasonable correlation appears to exist between the microscopic and specific gravity methods for the determination of volume fraction of porosity.

2. The total hydrogen content of weld pools shows a maximum with solidification time. This behavior depends upon the time available for the hydrogen pores to agglomerate and leave the melt.

3. Porosity nucleation shows comparable behavior, but with a minimum after solidification times of about 5 seconds. This seems to indicate that the pores form, agglomerate, and then leave the melt. This trend is reversed, after 5 seconds, by the formation of new pores which have some time to grow but do not have time to escape.

4. Porosity growth rate data seems to confirm this behavior by indicating a sharp increase in pore growth for the first 5 seconds which is then followed by a decrease in pore growth. This apparent decrease in pore-growth rate at longer solidification times probably is a result of longer times available for the escape of hydrogen.

5. The observed pore nucleation and growth rates explain the large amounts of fine porosity which obscured the X-rays and precluded measurements of the pore area fraction by this method.

6. The good, linear agreement of pore volume fraction as a function of the Johnson-Mehl parameter appears to provide reasonable assurance that the techniques employed as well as the resultant data are valid.

FUTURE WORK

The program indicated in Table 2 is being continued. The analytical work on these specimens is also being accelerated. Some additional specimens also will be tested to verify the data in the first nine experiments.

Work has also been started on the assembly of the test chamber for the welding of the bead-on-plate specimens.

REFERENCES

1. Saperstein, Z. P., and D. D. Pollock, "Porosity and Solidification in Aluminum Welds", Douglas Aircraft Co. Engineering Paper 3046, Presented to MSFC Aluminum Welding Symposium, Huntsville, Ala., July, 1964. (This paper contains a comprehensive list of references on the effects of hydrogen in aluminum welds.)

TABLE I

PHASE I BASIC DESIGN
(ALL MATERIAL IS 2219-T87)

Experiment No.	Block No.	Arc Atmosphere Contaminant Level	Arc Current Level	Arc Voltage Level	Arc Time Level	Material Thickness	
1	1	M	M	M	M	L	Center
2		L	L	L	L	L	
3		H	H	H	H	L	
4	2	H	H	H	L	H	
5		L	L	L	H	H	
6		H	H	L	H	H	
7		L	L	H	L	H	
8	3	L	L	H	H	L	
9		H	H	L	L	L	
10	4	M	M	M	M	L	Center
11		H	L	H	H	H	
12	5	L	H	L	L	H	
13		L	H	L	H	L	
14		H	L	H	L	L	
15		L	H	H	L	L	
16	6	H	L	L	H	L	
17		H	L	L	L	H	
18		L	H	H	H	H	
19	7	M	M	M	M	L	Center
20		H	M	M	M	L	
21		L	M	M	M	L	
22		M	H	M	M	L	
23	8	M	L	M	M	L	
24		M	M	H	M	L	
25		M	M	L	M	L	
26		M	M	M	H	L	
27		M	M	M	L	L	

L = Low, M = Medium, H = High

TABLE 2
SPECIMEN STATUS FOR PHASE 1 EXPERIMENTS

INDIVIDUAL TASKS

EXPERIMENT & SPECIMEN NO.	WELDING	X-RAYS (TOP)	MACROGRAPHS (TOP)	SECTIONING (1/8-IN)	X-RAYS (SIDE)	POLISHING	POROSITY COUNT	MACROGRAPHS OF NUGGET	MICROGRAPHS DENDRITE SPACING	NUGGET REMOVAL	SPECIFIC GRAVITY	HYDROGEN ANALYSIS
1												
1951	*	*	*	*	*	*	*			*		*
19103	*	*		*	*	*	*		*	*	*	
1912	*	*		*	*	●	*			*	*	
2												
191	*	*	*	*	*	*	*		*	*	*	
19125	*	*		*	*	*	*			*		●
19111	*	*		*	*	*	*		*	*	*	
3												
1962	*	*	●	*	*	*	*			*		*
193	*	*		*	*	*	*			*	*	
1924	*	*		*	*	*	*			*	*	
4												
A198	*	*	*	*	*	*	*		●	*	●	
A1926	*	*		*	*	*	*					
A1937	*	*		*	*	*	*			*		*
5												
A1922	*	*		*	*	*	*					
A193	*	*	*	*	*	*	*					
A1925	*	*		*	*	*	*					
6												
A195	*	*		*	*	*	*					
A1910	*	*		*	*	*	*		*	*	●	
A1923	*	*	*	*	*	*	*					
7												
A1935	*	*	*	*	*	*	*		●	*	*	
A1932	*	*		*	*	*	*					
A1915	*	*		*	*	*	*					
8												
19102	*	*		*	*	*						
19128	*	*		*	*	*	*		●			
1983	*	*	*	*	*	*	*			*		*
9												
198	*	*		*	*	*	*					
1981	*	*	*	*	*	*			*	*	*	
19112	*	*		*	*	*	*			*	*	*

* Denotes completion of task

TABLE 2 (Cont'd)

SPECIMEN STATUS FOR PHASE 1 EXPERIMENTS

INDIVIDUAL TASKS

EXPERIMENT & SPECIMEN NO.	WELDING	X-RAYS (TOP)	MACROGRAPHS (TOP)	SECTIONING (1/8-IN)	X-RAY (SIDE)	POLISHING	POROSITY COUNT	MACROGRAPHS OF NUGGETS	MICROGRAPHS DENDRITE SPACING	NUGGET REMOVAL	SPECIFIC GRAVITY	HYDROGEN ANALYSIS
10 1989 19121 1935	* * *	*	*	*	*	*	*			*	*	
11 A1919 A1921	* *	*	*	●	*	*	*					
12 A1938 A1941	* *	*	*	*	*	*	*					
13 1993 19127	* *	*	*	*	*	*						
14 1958	*	*	*	*	*	*	*					
15 19107	*	*	*	*	*	*						
16 1954	*	*	*	*	*	*	*					
17 A199	*	*	*	*	*	*	*					
18 A1927	*	*	*	*	●		*					
19 1995	*	*	*	*	*	●	●					
20 1920	*	*	*	*	*	*	**			●	*	

TABLE 2 (Cont'd)

SPECIMEN STATUS FOR PHASE 1 EXPERIMENTS

INDIVIDUAL TASKS

EXPERIMENT & SPECIMEN NO.	WELDING	X-RAYS (TOP)	MACROGRAPHS (TOP)	SECTIONING (1/8-IN)	X-RAYS (SIDE)	POLISHING	POROSITY COUNT	MACROGRAPHS OF NUGGETS	MICROGRAPHS DENDRITE SPACING	NUGGET REMOVAL	SPECIFIC GRAVITY	HYDROGEN ANALYSIS
21 1933	*	*	*	*	*	*						
22 1971	*	*	*	*	*	*	*			*	*	
23 1945	*	*	*	*	*	*	*					
24 1928	*	*	*	*	*	*	**			●	*	●
25 19 X	*	*	*	*	*							
25 1957	*	*	*	*	*							
27 19101	*	*	*	*	*	*	*					

TABLE 3

PRELIMINARY RESULTS, PHASE 1 (ALL MATERIALS 2219-T87)

EXPERIMENT & SPECIMEN NO.	WELDING* CONDITIONS	% POROSITY DETERMINED BY MICROSCOPE	% POROSITY DETERMINED BY SPECIFIC GRAVITY	Δt (SECONDS ± 0.25 SEC)	G AVERAGE (IN³/SEC X10-9)	N AVERAGE (PORES/SEC)	HYDROGEN (PPM, 0.01 ± 0.5%)	AVERAGE PORE RADIUS (INCHES)	DENDRITE SPACINGS (INTERSECTIONS/INCH AT 200X)
1	MMMM								
1951		13.79	N	2.25	7.65	911	24.7	0.0016	N
19103		5.40	7.14	2.75	2.03	955	--	0.0011	N
1912		10.84	4.93	2.75	4.17	1191	--	0.0014	9.6
2	LLLL								
191		0	0.014		0	0	--		7.6
19125		0	N		0	0	29.0		N
19111		0	0.53		0	0	--		12.5
3	HHHH								
1962		8.35	6.70	11.0	4.04	154	33.6	0.0022	N
193		15.30	6.99	12.5	4.07	230		0.0023	N
1924		14.95	5.40	11.5	3.38	174	27.8	0.0021	N
4	HHHL								
A198		4.03	4.92						N
A1926		2.43	N						N
A1937		4.16	N				45.0		N
5	LLLH								
A1922		.03	S		0	0	--		N
A193		0	S		0	0	--		N
A1925		0	S		0	0	--		N
6	HHLH								
A195		0.95	3.64	5.50	5.09	38	--	0.0020	N
A1910		2.72	3.69	9.25	4.81	59	--	0.0022	5.5
A1923		4.95	N	11.25	5.55	95	--	0.0025	N
7	LLHL								
A1935		0	+0.93		0	0	--		21.5
A1932		0	N		0	0	--		N
A1915		0	N		0	0	--		N
8	LLHH								
19128		0	0.09		0	0	--		16.1
19102		0	N		0	0	--		N
1983		0	N		0	0	53.0		N
9	HHLL								
198		7.25	7.74	5.0	3.43	479		0.0016	N
1981			5.34						N
19112		8.00	4.72	3.25	10.31	449	44.0	0.0020	4.4
24	MMHM								
1928		21.43	5.95	2.25	1.86	225		0.0010	

*	L	M	H	
Atmosphere	15	250	500	(PPM ± 5%)
Amperage	90	120	150	(AMPS ± 2 AMPS)
Arc Gap	0.030	0.060	0.090	(Inches ± 0.004-Inches)
Time	40	60	80	(Seconds ± 0.25 Sec.)

N = Not determined
S = Nugget too small to remove
Prefix "A" indicated 3/4" material, otherwise 1/4" material

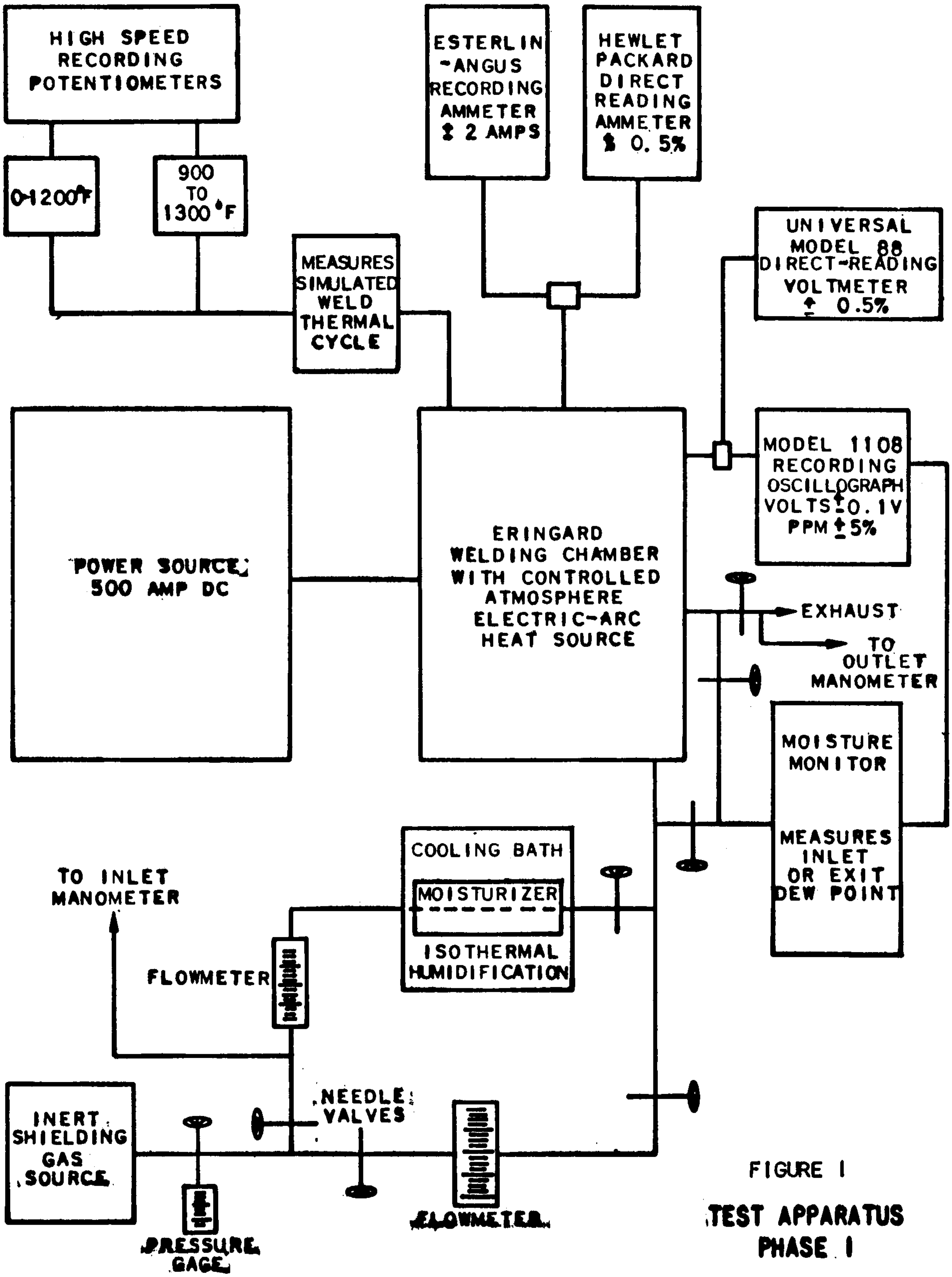

FIGURE 1

TEST APPARATUS
PHASE I

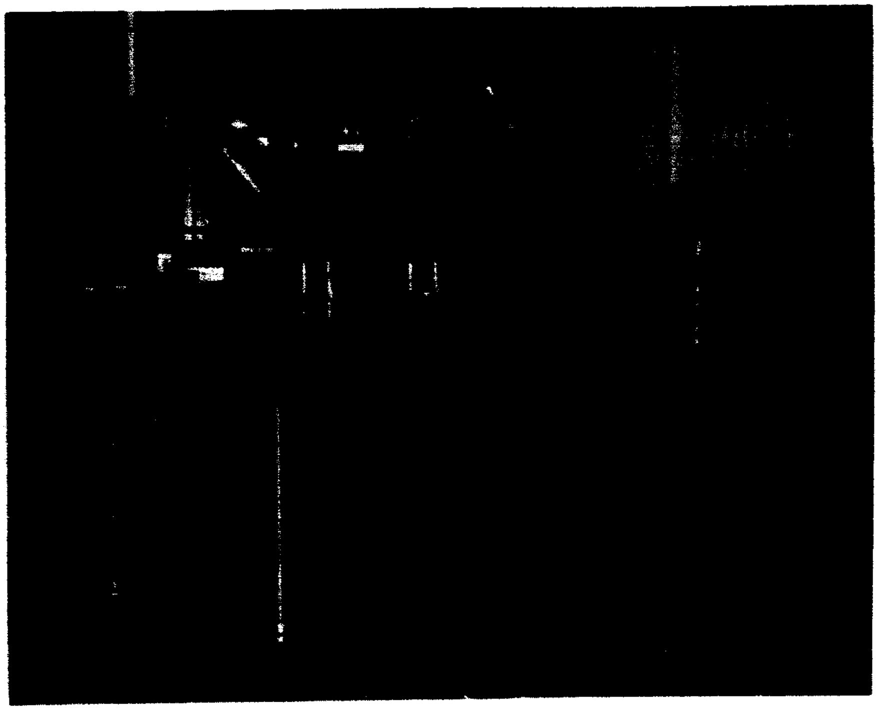

FIGURE 2

ERINGARD CHAMBER

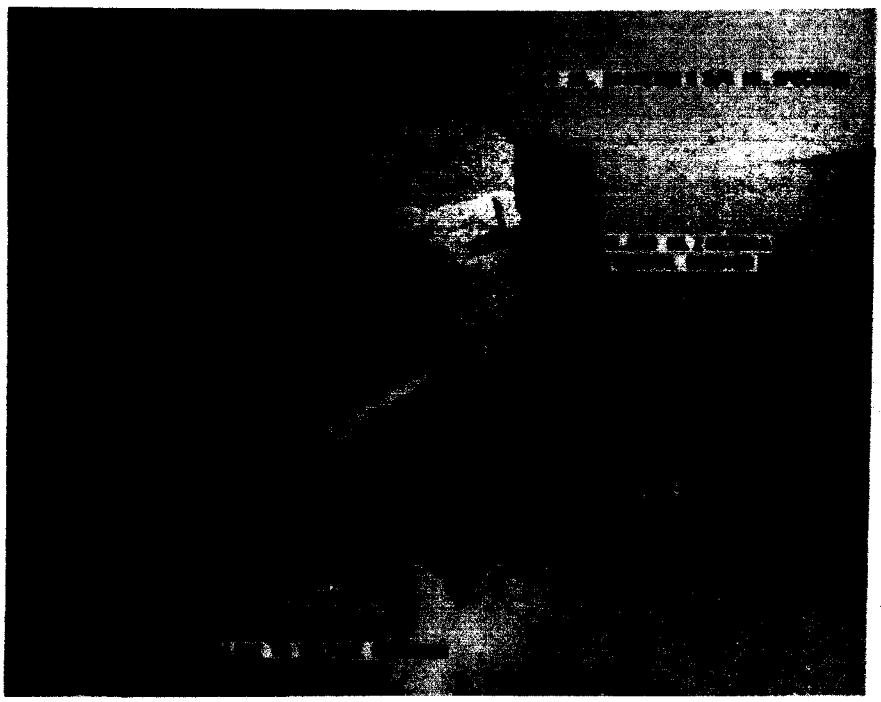

FIGURE 3

WELDING FIXTURE WITH SPECIMEN IN PLACE

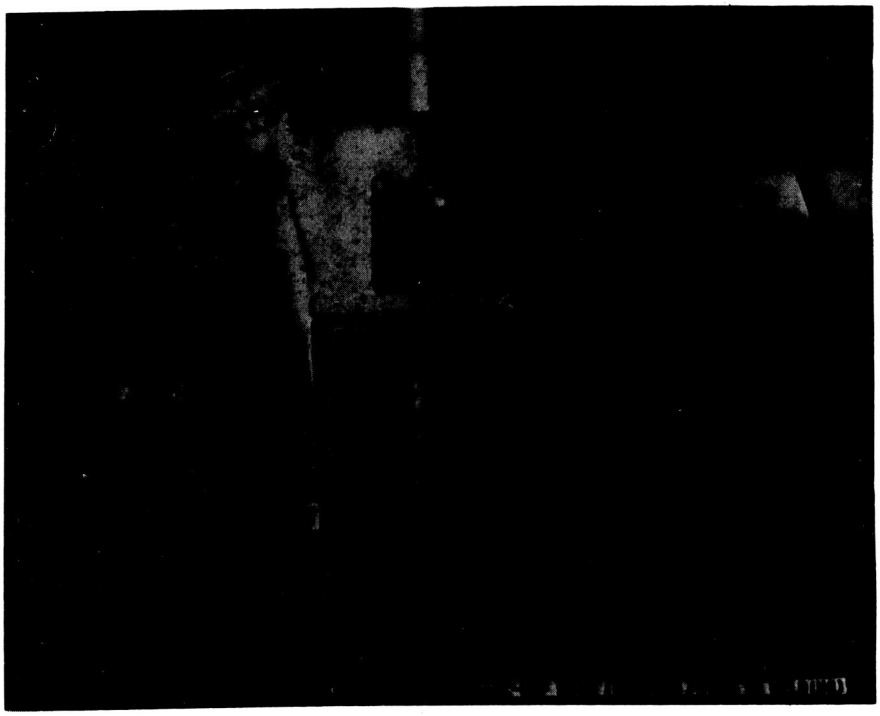

FIGURE 4

FIXTURE IN WELDING CHAMBER WITH SHIM IN PLACE

FIGURE 5

FIXTURE INSIDE CHAMBER PRIOR TO WELDING

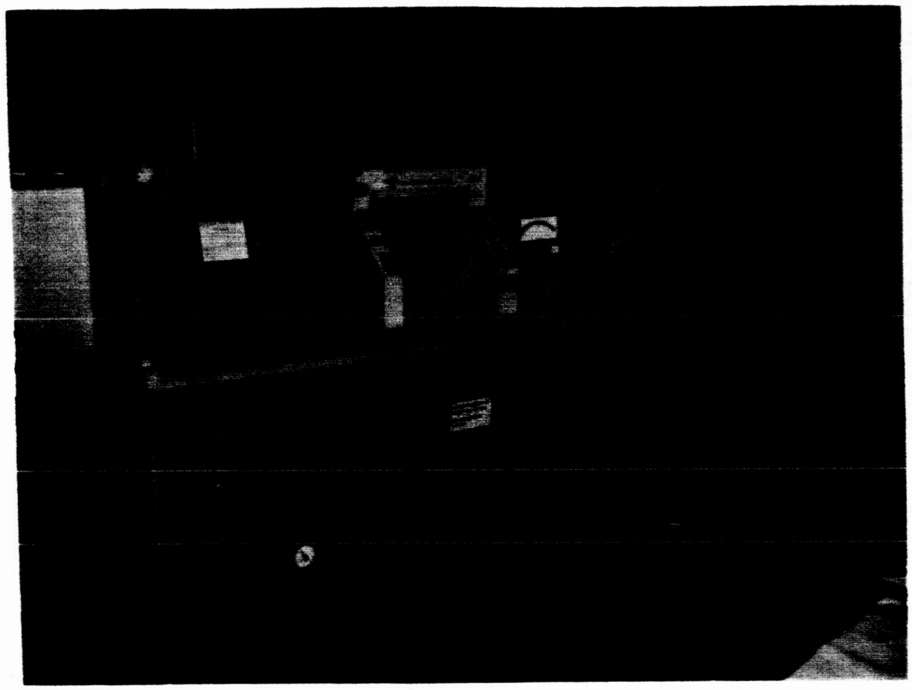

FIGURE 6

DEVICES TO MEASURE AND RECORD WELDING VARIABLES

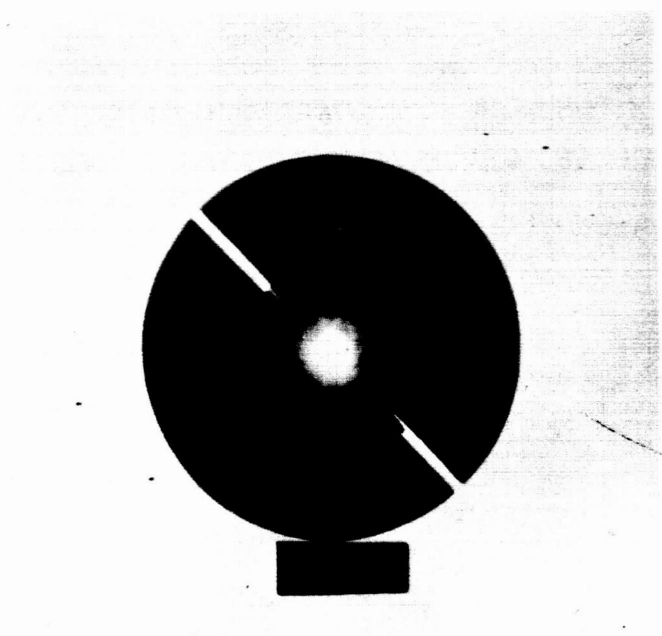

FIGURE 7

RADIOGRAPH OF TYPICAL 1/4-INCH SPECIMEN
SHOWING POROSITY AND LOCATION OF THERMOCOUPLE WIRES

FIGURE 8 - SKETCH OF A TYPICAL PORE COUNT

SPECIMEN 1928 2nd SIDE

#8 GRID - 2.5 OBJ.

% POROSITY

MICROSCOPIC = 21.95%

SPECIFIC GRAVITY = 6.67%

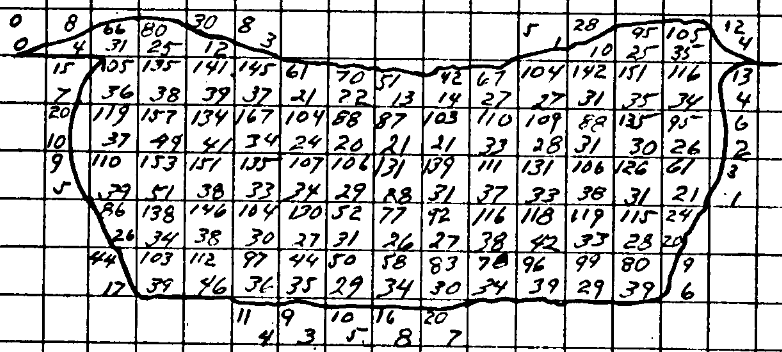

NUMBER OF PORES	52	530	766	714	667	455	376	420	479	482	563	582	702	410	34	= 7232	TOTAL
NUMBER OF CELLS COVERED	26	186	236	214	177	144	136	130	123	169	170	134	188	116	11	= 2160	TOTAL

AREA
OVERLAY = 4.27 sq in.

MAGN.: ONE No. 8 GRAIN SIZE GRID = 0.046"

0.046 in.

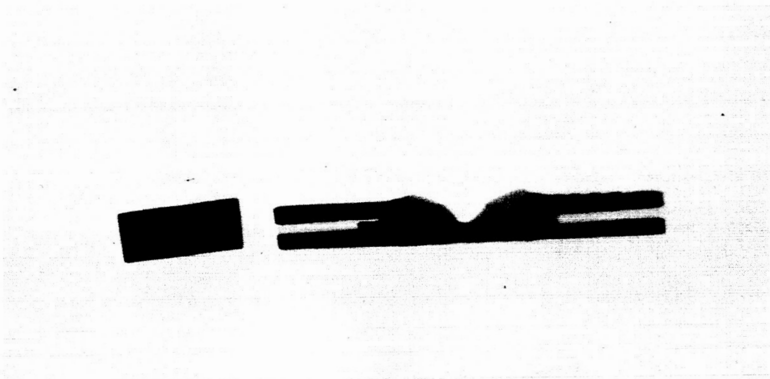

FIGURE 9

TRANSVERSE RADIOGRAPH OF TYPICAL 1/4-INCH THICK SPECIMEN

FIGURE 10

MICROGRAPH OF TYPICAL DENDRITE CELL STRUCTURE

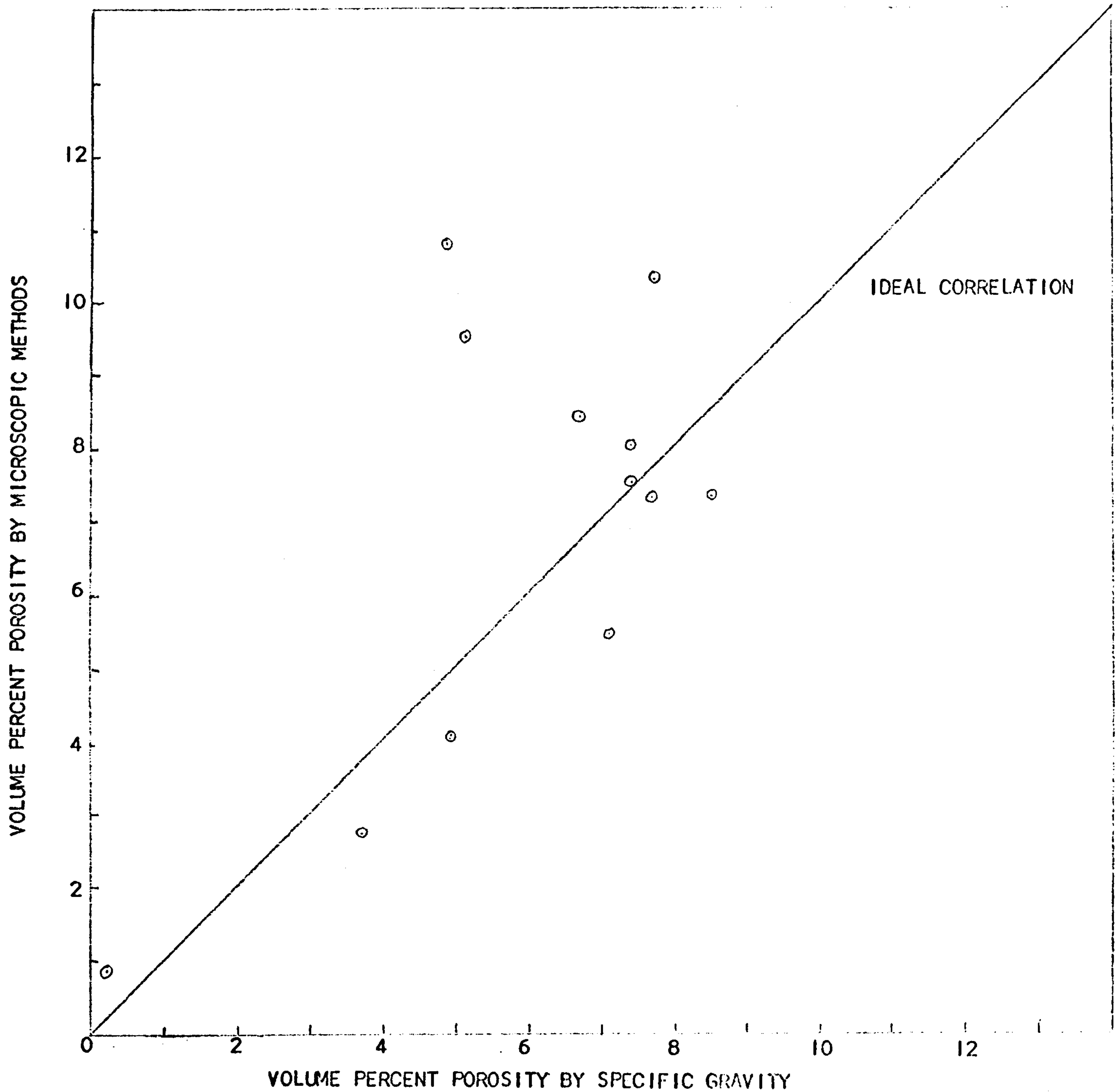

FIGURE 11 CORRELATION BETWEEN SPECIFIC GRAVITY AND MICROSCOPIC METHOD FOR VOLUME PERCENT POROSITY

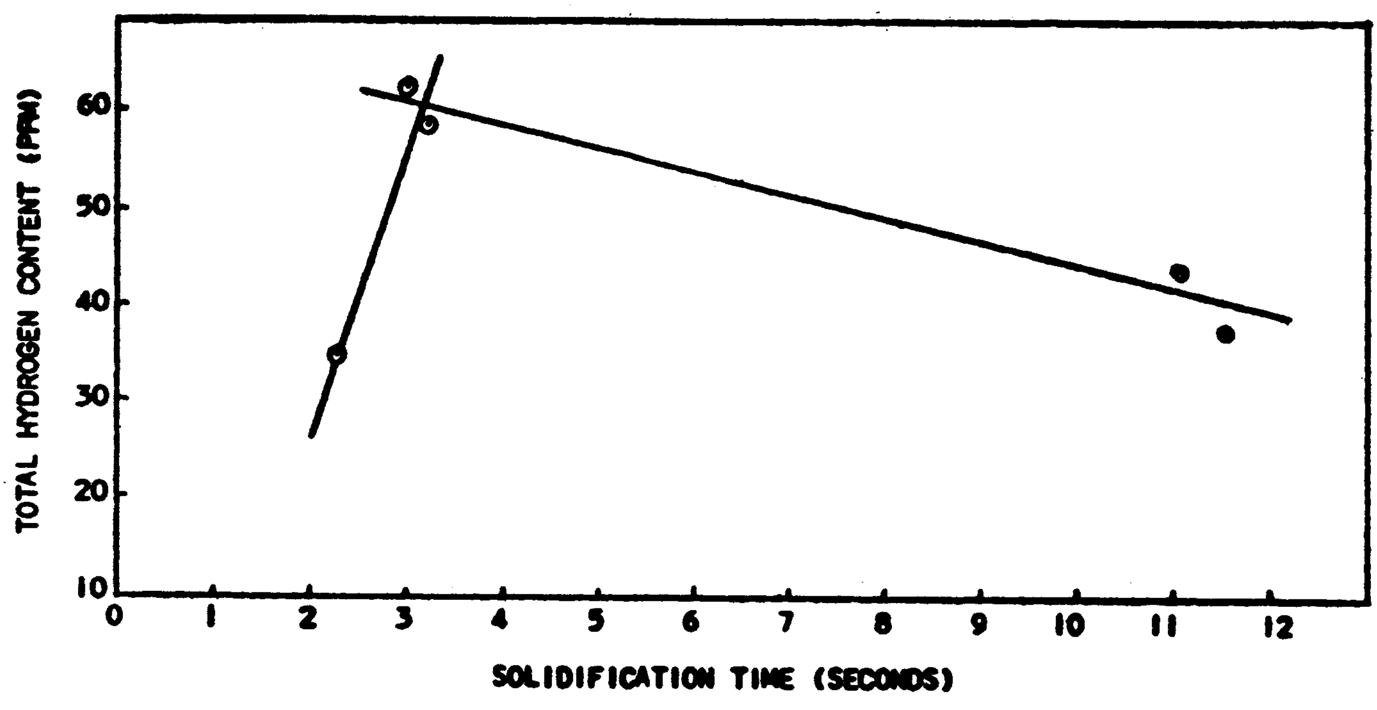

FIGURE 12 INFLUENCE OF SOLIDIFICATION TIME ON TOTAL HYDROGEN CONTENT

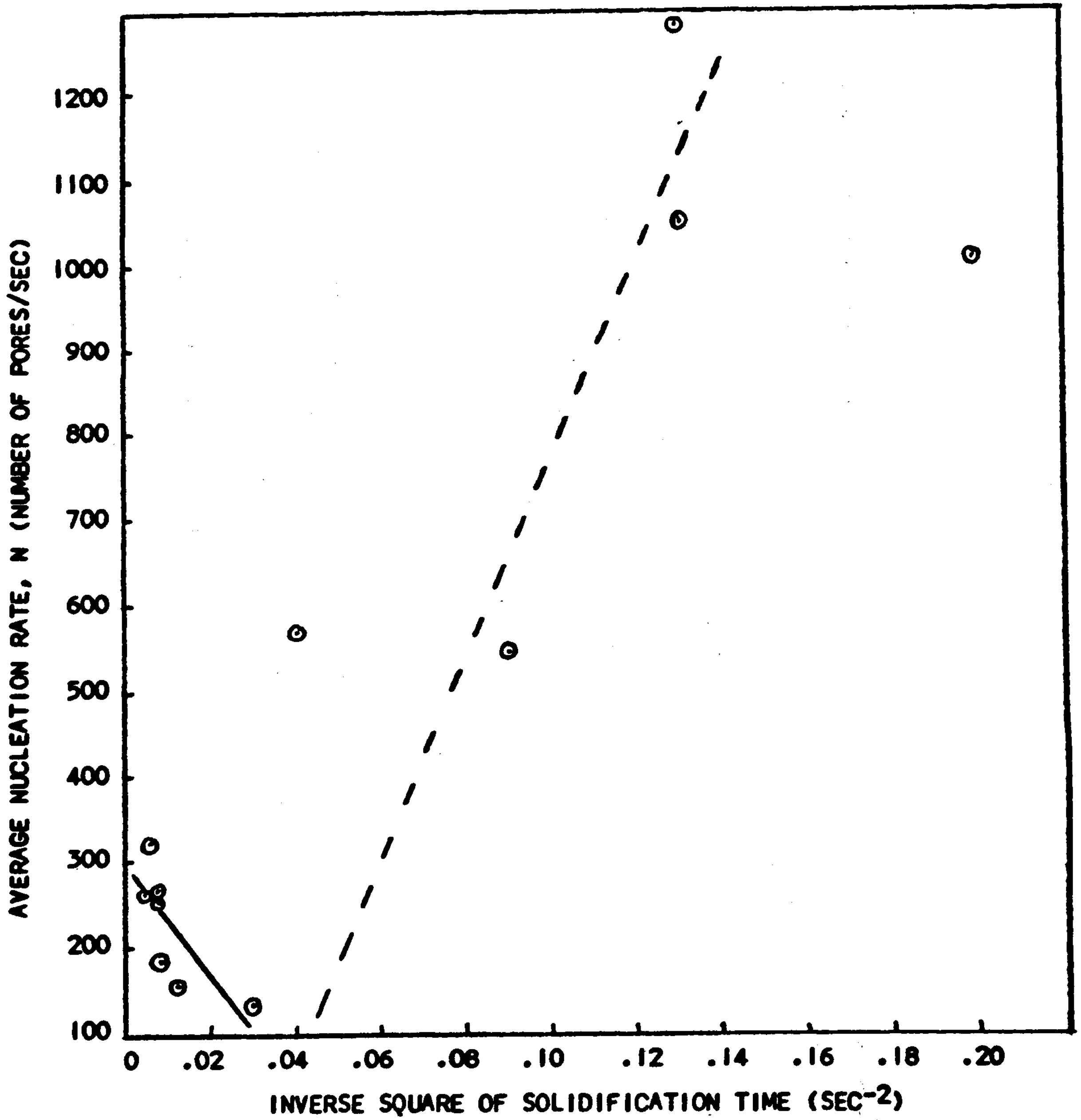

FIGURE 13 INFLUENCE OF SOLIDIFICATION TIME ON AVERAGE PORE NUCLEATION RATE

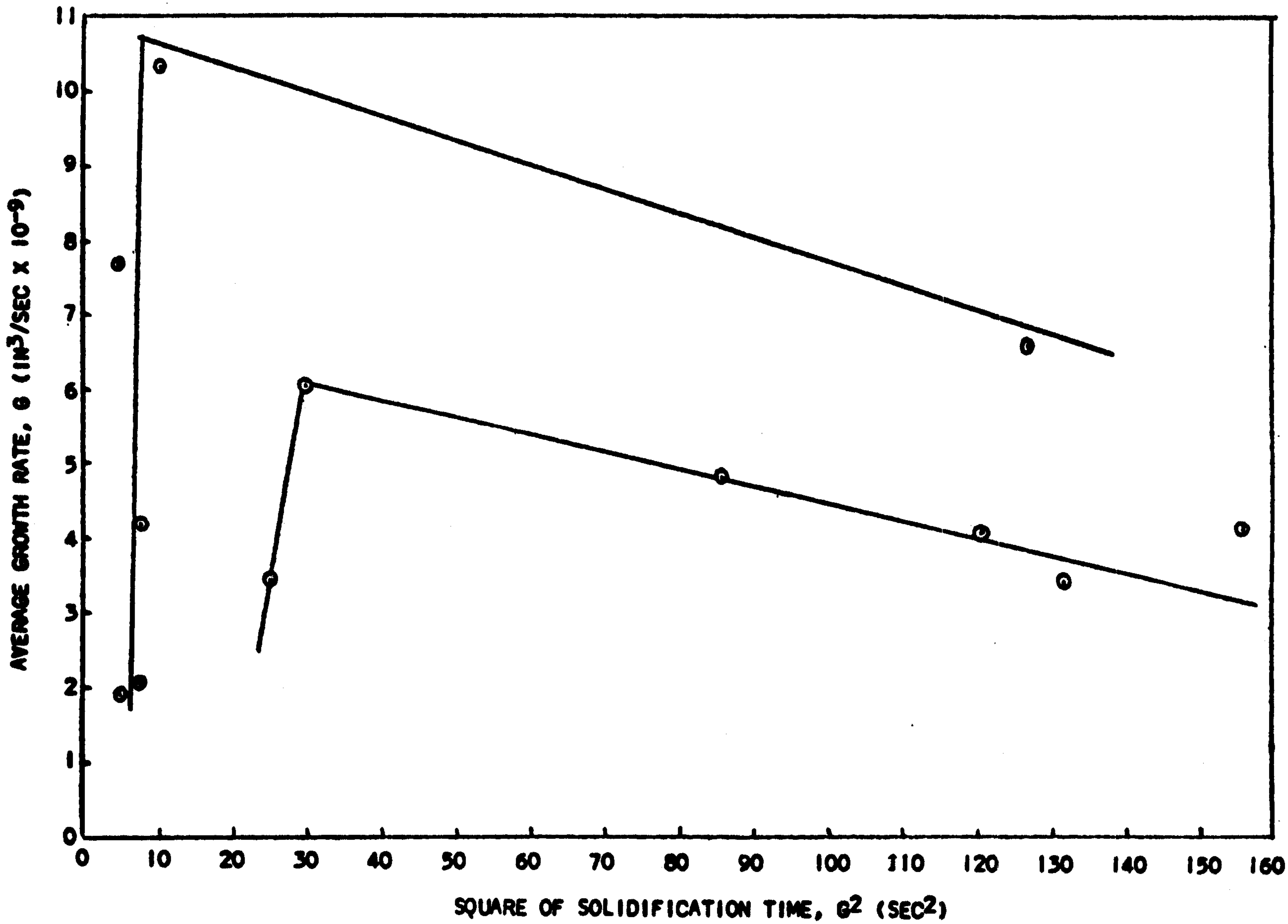

FIGURE 14 INFLUENCE OF SOLIDIFICATION TIME ON AVERAGE PORE GROWTH RATE

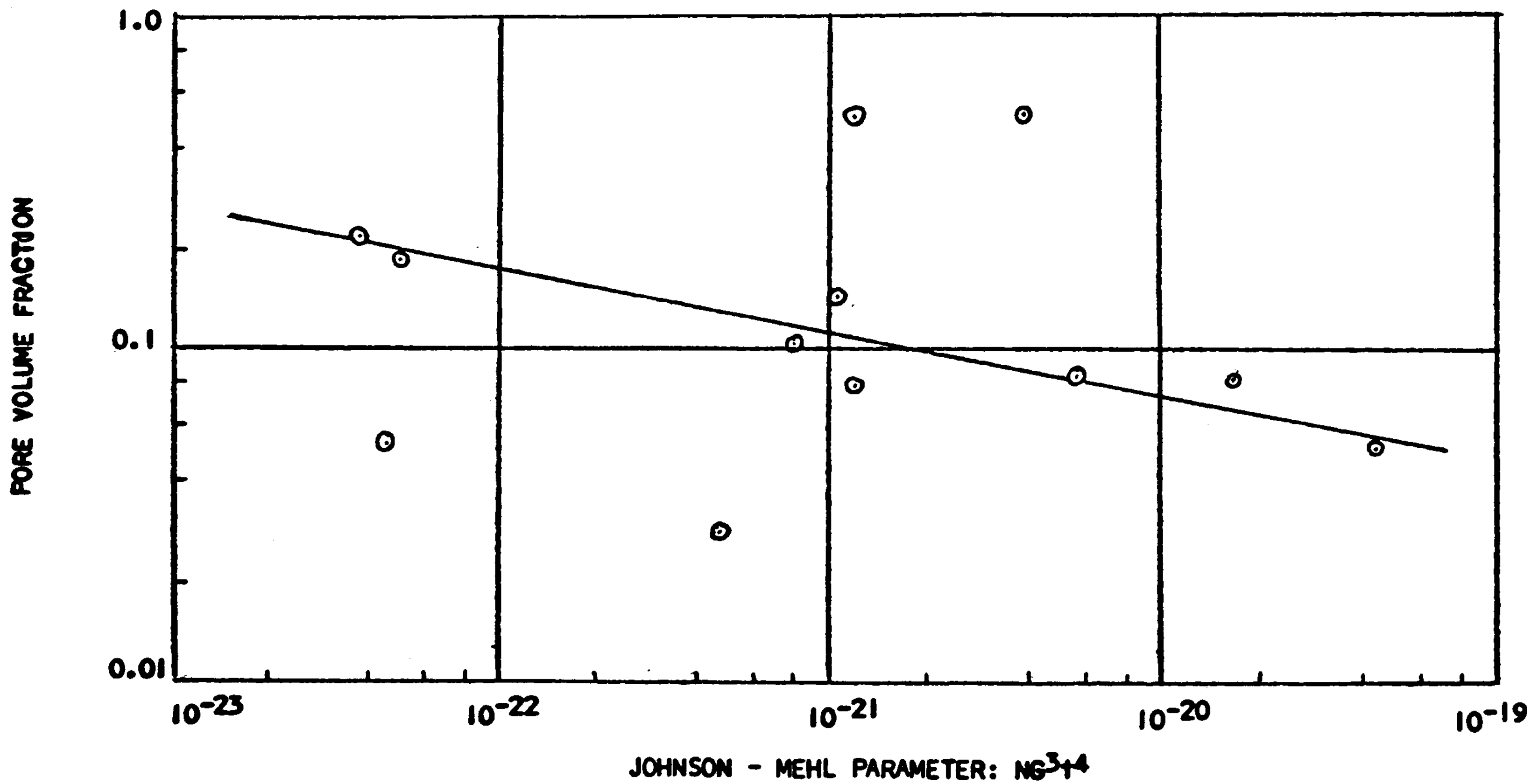

FIGURE 15 PORE VOLUME FRACTION AS A FUNCTION OF THE JOHNSON - MEHL PARAMETER

APPENDIX

POROSITY FORMATION AS A NUCLEATION AND GROWTH PROCESS

The evolution of gas from a melt is a process which is dependent upon two major mechanisms: the nucleation of stable agglomerations of gas molecules and the growth of such nuclei into bubbles, which appear as voids or porosity in the solidified matrix. Classical thermodynamics (Reference 12) may be used to demonstrate the factors affecting the two major parameters and to show how these may be used to explain observed, experimental behavior.

Nucleation

A stable nucleus of formerly dissolved gas will form when the Gibbs free energy (ΔF) becomes negative. This quantity may be expressed as the sum of component free-energies:

$$\Delta F = -\Delta F_m + \Delta F_s + \Delta F_c \tag{1}$$

where ΔF_m is the chemical free energy of the nucleating gas, ΔF_s is its surface free energy and ΔF_c is its strain energy. Since this work is primarily concerned with gas evolution in the liquid state, ΔF_c will be negligible. Under these conditions, ΔF_s sets the lower limit on the size of the stable nucleus. If ΔF_s is too large (molecular agglomeration too small), the nucleus will redissolve. If ΔF_s is small (molecular agglomeration large), the nucleus will grow.

Equation (1) may be rewritten as

$$\Delta F = -k_1 a^3 + k_2 a^2 \quad , \tag{2}$$

where k_1 is the chemical energy per unit volume and k_2 is the surface energy per unit area and a is the radius of the nucleating particle. The equilibrium nucleus size derived from equation (2) is found to be

$$a_o = \frac{2}{3} \frac{k_2}{k_1} \tag{3}$$

and the change in free energy thus becomes

$$\Delta F = \frac{4}{27}\frac{k_2^3}{k_1^2} \tag{4}$$

The smallest stable nucleus that will form an observable void in a eutectic system, such as under consideration in this work, is that which forms at the eutectic temperature and has sufficient time to grow. Under these conditions, the equilibrium nucleus size, a_o of equation (3), will be a constant, and equation (3) may be employed to reexpress equation (4) as

$$\Delta F = \text{Const. } k_2 \tag{5}$$

Thus, the change in free energy will be an inverse function of the radius (r) of the particle as given by

$$\Delta F = \text{Const. } \frac{1}{r^2} \tag{6}$$

since the surface energy varies inversely as the area of the gas nucleus.

In the liquid state considered here, the diffusion of the gas atoms through the liquid to the growing nuclei will be relatively unimpeded (Reference 13). The nucleation rate, N, may be approximated by

$$N = \text{Const. } \exp^{-\Delta F/RT} \tag{7}$$

However, the temperature at the eutectic is constant until solidification is completed, so that equation (7) may be rewritten (using equation (6) and a series approximation for e^x) as

$$N = \frac{\text{Const.}}{r^2} \tag{8}$$

Pore Growth

Equation (8) provides an approximation of the rate of nucleation of the smallest observable gas bubbles which grow at the eutectic temperature. The rate of growth, G, of these bubbles must now be described. The growth rate of a sphere is given by (Reference 14)

$$G = \frac{dV}{dt} = 4\pi r^2 \frac{dr}{dt} \tag{9}$$

where V is the volume of the growing bubble and t is the time. At a given temperature, the eutectic temperature, the bubbles may be assumed to grow at an essentially constant rate. Expressed mathematically,

$$dr = \text{Const.}\ dt \tag{10}$$

Integration of this equation gives

$$r = \text{Const.}\ (t - t_E) \quad , \tag{11}$$

where t_E is the time of growth at the eutectic temperature. For a given aluminum alloy composition subjected to a given amount of superheating, t_E will be very nearly a constant value. Thus, all bubbles which grow larger than what was previously defined as the smallest observable bubble will have radii that are a direct function of the time that the molten material was allowed to grow at temperatures above the eutectic.

Equation (11) may also be employed to provide further insight into the nucleation rate as given by equation (8); this becomes

$$N = \frac{\text{Const.}}{(t - t_E)^2} \tag{12}$$

Thus, the nucleation rate is shown to be inversely proportional to the time that the melt is kept above the eutectic temperature — in agreement with observed behavior.

In applying equation (11) to equation (9), the growth rate may be rewritten as

$$G = \text{Const. } (t - t_E)^2 \tag{13}$$

Integration of both sides of this equation with respect to time, between the limits of t_E and t, gives

$$\int_{t_E}^{t} G dt = \text{Const. } (t - t_E)^3 \tag{14}$$

This is an expression for the total volume of all bubbles at an initial time, t. The total volume of voids grown after that is

$$df \doteq \left[\int_{t_E}^{t} G dt\right] N\,(1 - f)\, dt \quad , \tag{15}$$

where f is the fraction of the gas that is contained in the bubbles. When equation (15) is integrated and equation (12) is substituted for N,

$$f = \frac{\text{Const.} t^4}{(t - t_E)^2} \tag{16}$$

Thus, the fraction of the gas that has precipitated from the melt and coalesced to form bubbles is primarily a function of the time that the melt spent above the eutectic temperature. To a first approximation, equation (16) may be shown schematically as in Figure 2-10, where most of the bubble formation occurs before t_E. The volumetric fraction of porosity is also expressed by equation (16), except that the proportionality constant is different.

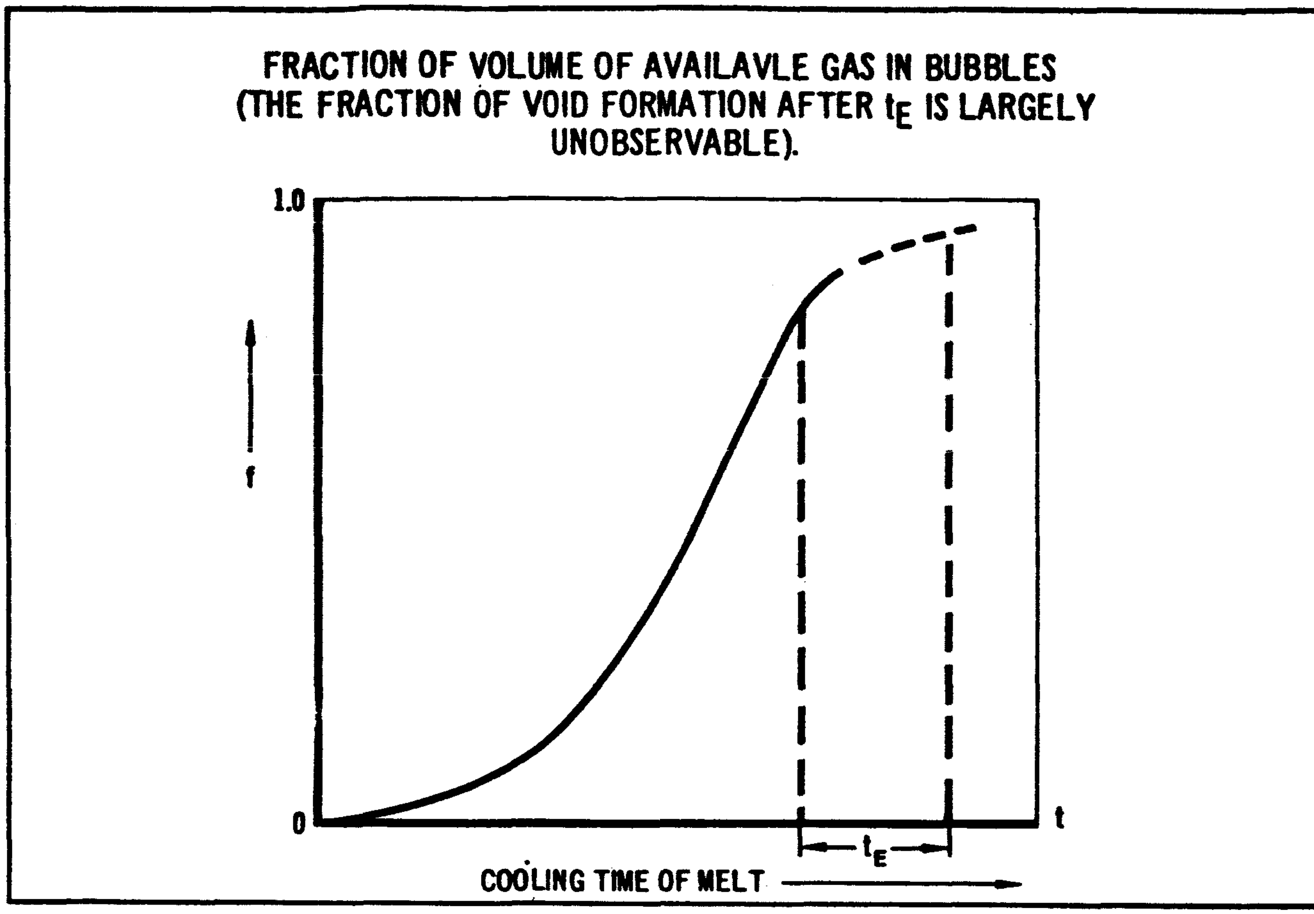

FIGURE 2-10

Pore Size

The expressions for N and G, equations (12) and (13), permit the calculation of the average void size, s, since

$$s = \text{Const.} \left(\frac{G}{N}\right) \tag{17}$$

Upon substitution, equation (17) becomes

$$s = \text{Const.} \ (t - t_E)^4 \tag{18}$$

or the average bubble size is directly proportional to the fourth power of the time that the melt is above the eutectic temperature.

In this analysis of the formation and growth of pores in molten alloys, it will be noted that all of the significant parameters necessary for the understanding of this reaction have been reduced in terms of time spent at or above the

eutectic temperature. This is important because these factors may be measured with a high degree of accuracy, and the equations are thus more valid than those with some less accurately determinable parameters. Another important point is that the use of such time factors automatically provides that the parameters affecting bubble formation will be sensitive to the rate of heat transfer from the molten alloy. In other words, since the time for solidification is a function of the temperature difference between the molten metal and the surrounding solid material, the mechanism of porosity formation may be a function of the time-temperature cycles.

A similar set of equations may be derived in terms of the initial temperature of the melt and the eutectic temperature of the alloy. Such an analysis would not be as helpful in understanding these phenomena as that just given, because it does not account for the rate of heat removal.

The analysis presented here implicitly assumes that all of the gas ejected from the melt will be retained as pores in the solidified weld and that none of it would float to the surface. It also considers that no pores will form after solidification. When such factors are taken into consideration with the simplifications made in the mathematical analysis, it is apparent that the experimental data will deviate somewhat from the theoretically predicted behavior. Where significant deviations do occur, these will be explained in terms of the parameters affecting the phenomenon in question. The behavior predicted by the equations does agree with observed behavior, provides an insight into the mechanism of porosity formation, and furnishes a guide to the experimental verification of this phenomenon.

REPORT NO. 8

DATED 15 February 1965

LOCKHEED AIRCRAFT CORPORATION
GEORGIA DIVISION - MARIETTA, GEORGIA

TITLE

NAS 8-11435

A STUDY OF INERT-GAS WELDING
PROCESS TRANSFERABILITY OF SET-UP
PARAMETERS

PROGRESS REPORT
15 February 1965
Report No. 8

PREPARED BY:	R. H. Kilpatrick	GROUP	Manufacturing Research
CHECKED BY:	E. R. Seay ERS	APPROVED BY	
APPROVED BY:	R. C. Stewart RCS Department Manager	APPROVED BY	

NAS 8-11435

PROGRESS REPORT

15 February 1965

OBJECT:

The object of this program is to establish extreme confidence in transferring weld settings and data from machine to machine and facility to facility.

PROCEDURE:

Equipment

Welding Unit No. 1 (Universal Test Jig)

Power	- Sciaky Model S-6 functional control 600 amperes d-c welding power source.
Head	- Airco Model HME-E automatic head for the gas tungsten arc welding process.
Carriage	- Lockheed developed all-position boom and carriage mounted on a Webb weld positioner. The carriage is controlled by a Servo-Tech tachometer feedback governor.
Wire Feed	- Airco Model AHF-B feed rolls with Airco Model AHC-B feed-back type governor control.
Instrumentation	- Texas Instrument "Servo/riter" 4 channel potentiometric recorder.

Welding Unit No. 2 (Test Bed)

Power	- Sciaky Model S-6 functional control 600 amperes welding power source.
Head	- Precision Sciaky (MIG) (TIG) welding head with proximity head control.
Carriage	- Servo-Tech control system to operate a Lockheed designed carriage.
Wire Feed	- Airco AHC-B wire feed control with tachometer feedback governor.
Instrumentation	- Minneapolis-Honeywell "Electronic 17" four channel potentiometric recorder.

The analysis of significance of the variables and the regression analysis is being run on Unit No. 1.

Unit No. 1 and Unit No. 2 are to be used for transferability.

Experimental Design:

The experimental design used during the development program to determine the significance of the variables and to establish response characteristics is a 1/16 replication of nine factors in eight blocks of four units each. This design is being used completely randomized with several two factor interactions measurable. (See pages 5 and 6.)

Welding Variables:

The following variables (independent) have been chosen for consideration during the TIG portion of the development. (See pages 7, 8, and 9.)

C = Welding current, recorded so that each chart line (2.5 mm) is equal to 0.5 amps.

V = Welding voltage, recorded so that each chart line (2.5 mm) is equal to 0.05 volts.

T = Welding travel speed, recorded so that each chart line is equal to 0.5 in/min or 0.2 in/min.

Ws = Filler wire speed, recorded so that each chart line is equal to 1.0 in/min or 0.2 in/min.

Wd = Volume of filler wire deposited (in^3/inch of weld). This is calculated from weld travel and wire speed and entered directly as a weld variable on the computer data sheets.

Gp = Inert shielding gas (Helium) purity measured in parts per million total impurity. The high impurity gas for the experiment has been contaminated with air to produce high, medium, and low impurity gas as follows:

Impurity-ppm	N_2	H_2O	O_2	Butane	Total ppm
Low impurity	15	4	2	1	22
Medium impurity	60	8	12	1	81
High impurity	110	13	25	1	149

Gf = Shielding gas flow rate (cfh) using calibrated flow gages. Helium is being used throughout the TIG program.

°f = Temperature of the weldment prior to welding. This is controlled using a direct reading contact pyrometer to determine uniformity and temperature level.

J = Weld joint spacing or gap measured in inches. Shims are used during the specimen tack weld operation to control the joint gap.

D = Diameter of the electrode tip measured in inches. The 3/16 thorated tungstens electrodes are machine ground with 2.4° taper and then blunted to the desired tip diameter.

The torch resistance variable is under control by the use of the Lockheed, high amperage, low resistance torch.

Responses or Dependent Variables

Ftu = Ultimate Tensile Strength

Fty = Yield Strength 2% Offset

e = Elongation, % of 2 inches.

M = Cross section area of the apparent melt zone as measured from specimen macrographs.

H = Cross section area of apparent heat affected zone as measured from specimen macrographs.

P = Depth of penetration of melt as measured from the top surface of the specimen.

Q = Overlap in melt penetration when specimen is welded from both sides.

E = Electrical energy of the welding arc in joules per inch of weld.

M_t = Temperature envelope as recorded from Cramel Alumel thermocouple taped to
T_t the back side and in the center of the weld joint. This envelope data is
A_t transferred to computer data sheets as maximum temperature, time above 450°F, and area under the curve above 450°F.

X = Radiographic. Porosity in the weld is measured by using a grid system that provides a porosity level from 0 to 100% over ten inches of weld. This number is applied directly to the computer data input.

Present Status

The computer analysis of the data from the 1/4" TIG is being accomplished. This is to include the analysis of variance, the regression analysis, the solution of the quadratic equations from the regression analysis and the plotting of selected response surfaces and parameters.

Prepared	NAME: RHKilpatrick	DATE: 1Nov 64	LOCKHEED-GEORGIA COMPANY A DIVISION OF LOCKHEED AIRCRAFT CORPORATION	Page 5	TEMP.	PERM.
Checked			TITLE Experimental Design TIG welding Analysis of Variance & Regression	Model		
Approved				Report No. 8		

Weld No 3/4	Weld No 1/4	Weld Number	C	V	T	Wd	Gr	Gf	°F	J	D
#153ST	U79ST	1	L	L	L	H	L	H	L	L	H
154	83	2	H	L	L	H	L	H	H	H	L
155	85	3	M	M	M	M	M	M	M	M	M
156	87	4	L	L	L	L	H	H	L	H	L
157	89	5	L	H	L	L	H	L	L	L	H
158	91	6	L	L	H	H	H	L	L	H	H
159	93	7	H	L	L	L	H	H	H	L	H
160	95	8	L	H	H	L	L	H	L	H	H
161	97	9	H	H	L	H	L	L	H	L	H
162	99	10	M	M	M	M	M	M	M	M	M
163	101	11	L	H	L	H	H	H	H	H	H
164	103	12	L	H	H	L	H	L	H	H	L
165	105	13	H	L	L	L	L	L	L	L	L
166	107	14	L	L	L	H	H	L	H	L	L
167	109	15	L	H	L	L	L	H	H	L	L
168	111	16	H	H	H	H	L	L	L	H	L
169	113	17	L	H	H	H	L	L	H	L	H
170	115	18	L	L	L	L	L	L	L	L	L
171	140	19	L	L	H	L	H	H	H	L	H
172	119	20	M	M	M	M	M	M	M	M	M
173	121	21	H	H	H	L	L	H	H	L	L
174	123	22	H	H	L	H	H	H	L	L	L
175	125	23	L	H	H	H	H	H	L	L	L
	127	24	H	L	H	L	L	L	H	H	H
	128	25	L	L	H	H	L	H	H	H	L
	129	26	M	M	M	M	M	M	M	M	M
	130	27	L	L	H	L	L	L	L	L	L
In Work	131	28	H	H	H	L	H	L	L	L	H
	132	29	H	L	H	H	L	H	L	L	H
	133	30	H	L	H	H	H	L	H	L	L
	134	31	L	L	L	L	L	L	H	H	H
	135	32	H	L	L	H	H	L	L	H	H
	136	33	H	L	L	H	H	L	H	H	L
	137	34	H	L	H	L	H	H	L	H	L
	138	35	L	L	L	H	H	L	L	H	L
	139	36	H	H	L	L	L	H	L	H	H

GA FORM 362-2

Prepared	NAME	DATE	LOCKHEED-GEORGIA COMPANY A DIVISION OF LOCKHEED AIRCRAFT CORPORATION	Page 6	TEMP.	PERM.
Checked			TITLE Measurable Two Factor Interactions	Model		
Approved				Report No. 8		

Interactions			Code
Voltage	-	Travel Speed	V T
Voltage	-	Current	V C
Wire Deposit	-	Travel Speed	Wd T
Wire Deposit	-	Current	Wd C
Gas Purity	-	Travel Speed	Gp T
Gas Purity	-	Current	Gp C
Gas Flow	-	Travel Speed	Gf T
Gas Flow	-	Current	Gf C
Electrode Dia	-	Travel Speed	D T
Electrode Dia	-	Current	D C
Work Temp	-	Travel Speed	°F T
Work Temp	-	Current	°F C
Joint Gap	-	Travel Speed	J T
Joint Gap	-	Current	J C
Current	-	Travel Speed	C T

GA FORM 362-2

Prepared	E H Kilpatrick	1 Nov 64	LOCKHEED-GEORGIA COMPANY A DIVISION OF LOCKHEED AIRCRAFT CORPORATION	Page 7	TEMP.	PERM.
Checked			TITLE Weld Parameters	Model		
Approved				Report No. 8		

Tungsen Arc Weld
2219-T87 Alloy
1/4 inch Thick

	Code Letter	High	Medium	Low	Units for Computer
Arc Current	C	2.85	2.73	2.60	Amp. ÷ 100
Arc Voltage	V	12.75	12.5	12.25	Volts
Travel Speed	T	23	21	19	IPM
Wire Deposit / in. of weld	Wd	1.228	.955	.682	$in.^3 \times 100$/in.
Gas Purity	Gp	1.50	.90	.30	ppm ÷ 100
Gas Flow	Gf	1.25	1.00	.75	scfh ÷ 100
Indicated Flow		154	121	88	
Work Temperature	°F	1.50	1.13	.75	°F ÷ 100
Joint Gap	J	.020	.010	0	in.
Electrode Tip Diameter	D	.125	.108	.090	in.

GA FORM 362-2

Prepared	NAME: RHKilpatrick	DATE: 26 Jan 65	LOCKHEED-GEORGIA COMPANY A DIVISION OF LOCKHEED AIRCRAFT CORPORATION	Page 8	TEMP.	PERM.
Checked			TITLE Weld Parameters Tungsten Arc	Model		
Approved				Report No. 8		

Tungsten Arc Weld
2219-T87 Alloy
3/4 Inch Thick

	Code Letter	High	Medium	Low	Units For Computer
Arc Current	C	4.40	4.20	4.00	Amp ÷ 100
Arc Voltage	V	12.2	11.85	11.5	Volts
Travel Speed	T	10	9	8	ipm
Wire Deposit/in. of weld	Wd	.3835	.1817	0	in^3 x 100/in
Gas Purity	Gp	1.50	.90	.30	ppm ÷ 100
Gas Flow	Gf	1.25	1.00	.75	scfh ÷ 100
Indicated Flow		154	121	88	
Work Temperature	°F	1.50	1.13	.75	°F ÷ 100
Joint Gap	J	.020	.010	0	inch
Electrode Tip Diameter	D	.135	.122	.108	inch

GA FORM 362-5

Sheet 1 of 4

Decl. No. 214.000

TRANSMITTAL FOR DIGITAL COMPUTATION

D.T.S. ________ RETURN TO ________________

	WELD NO. / m $Z13$	C $Z1$ / Mc $Z14$	V $Z2$ / Mf $Z15$	T $Z3$ / H $Z16$	W_o $Z4$ / P $Z17$	G_p $Z5$ / B $Z18$	G_f $Z6$ / E_p $Z19$	°F $Z7$ / X $Z20$	J $Z8$ / M_t $Z21$	D $Z9$ / T_f $Z22$	F_{tu} $Z10$ / A_t $Z23$	F_{ty} $Z11$	e $Z12$
	U73[illegible]	[illegible]	12.25	19.5	.646	1.49	.75	1.50	.020	.[illegible]	37.13	25.3	3.66
	.114	.[illegible]	.012	.164	.256	.023	-.030	20					
1	U798T	[illegible]	12.25	19.25	1.211	.11	1.25	.76	0	.125	18.6	18.5	2.66
	.071	.[illegible]17	0	.134	.193	.063	.052	2	11.35	13.13	1.71		
2	U835[illegible]	2.[illegible]	12.25	19.25	1.228	.14	1.25	1.50	.020	.090	38.1	23.3	4.00
	.103	.[illegible]	.010	.160	.287	.033	.018	1					
3	U85[illegible]	[illegible]	12.50	21.	.944	.81	1.00	1.13	.005	.108	28.8	23.9	3.00
	.077	.011	.005	.151	.260	.047	.045	10	7.50	4.38	.22		
4	[illegible]	2.61	12.25	19.6	.646	1.49	1.25	.75	.020	.[illegible]	39.0	24.7	3.33
	.[illegible]	.00[illegible]	.011	.161	.276	.023	.[illegible]	3	12.03	11.25	.19		
5	[illegible]	[illegible]	12.75	19.6	.646	1.49	.[illegible]	.75	0	.125	36.1	23.8	3.00
	.[illegible]	.[illegible]	.009	.164	.293	.[illegible]3	.063	4	9.22	9.38	.61		
6	U71[illegible]	2.[illegible]0	12.25	22.	1.316	1.4[illegible]	.75	.75	.020	.125	24.0	25.0	2.00
	.[illegible]	.013	0	.119	.183	.[illegible]	.074	0	4.4[illegible]	11.25	.19		
7	[illegible]	2.[illegible]	12.25	19.6	.646	1.49	1.25	1.50	0	.125	40.0	24.1	4.00
	.[illegible]	.011	.0[illegible]2	.147	.257	.030	.032	0	11.14	24.40	[illegible]		
8	U[illegible]T	2.60	[illegible].75	23.2	.6[illegible]	.14	1.25	.75	.015	.125	17.0	17.7	2.00
	.0[illegible]	.016	0	.126	.[illegible]5	.033	.019	5	8.11	5.0	[illegible]		
9	U9[illegible]T	2.5[illegible]	12.75	19.1	1.211	.14	.75	1.50	0	.125	39.0	23.7	4.[illegible]
	.095	.01[illegible]	.[illegible]	.186	.[illegible]53	.043	.052	10	11.40	22.50	2.57		
10	[illegible]	2.73	12.50	21.	.[illegible]44	.81	1.00	1.13	.011	.10[illegible]	35.8	24.4	3.33
	.0[illegible]	.011	.0[illegible]	.165	.276	.[illegible]	.048	7	10.15	6.88	.74		
11	[illegible]	2.00	12.[illegible]	19.	1.228	1.49	1.25	1.50	.20	.125	32.1	24.5	2.66
	.[illegible]	.011	.00[illegible]	.146	.293	.037	.072	5					
	← omit →												

GA Form GD928-1

Deck No. 3314.000

TRANSMITTAL FOR DIGITAL COMPUTATION

D.T.S. ______ RETURN TO ______

	Weld No. / M Z13	C Z1 / Mc Z14	V Z2 / Mf Z15	T Z3 / H Z16	Wd Z4 / P Z17	Ge Z5 / B Z18	Gc Z6 / Ep Z19	F Z7 / X Z20	J Z8 / Im Z21	D Z9 / Tt Z22	Ftu Z10 / At Z23	Fty Z11	Z12
12	41035T	2.60	12.76	23.2	.660	1.49	.75	1.50	.016	.010	33.5	23.8	2.00
	.074	.016	.002	.121	.260	.040	.053	8	—	—	—	—	—
13	2165ST	2.85	12.25	19.1	.646	.14	.75	.75	0	.090	39.7	26.3	[illegible]
	.100	.007	.011	.171	.283	.023	.024	0	13.26	11.88	2.07	—	—
14	U107ST	2.60	12.25	19.	1.228	1.49	.75	1.50	0	.090	38.6	26.1	3.33
	.071	.012	.014	.155	.293	.036	.043	21	13.57	16.25	3.46	—	—
15	[illegible]9ST	2.60	12.75	19.	.709	.14	1.25	1.50	0	.110	38.9	24.9	3.00
	.086	.015	.004	.158	.280	.030	.033	8	[illegible].50	[illegible]	1.18	—	—
16	U111ST	2.85	12.75	22.9	1.240	.14	.75	.75	.018	.070	32.8	26.7	2.00
	.077	.020	.005	.141	.270	.005	.058	6	6.47	3.13	.17	—	—
17	[illegible]13ST	2.60	12.75	22.8	1.228	.14	.75	1.50	0	.120	15.4	14.7	2.00
	.055	.012	0	.142	.186	.056	.084	2	4.090	3.13	1.23	—	—
18	[illegible]15ST	2.60	12.25	19.5	.646	.14	.75	.75	0	.090	40.4	26.0	4.00
	.054	.012	.005	.157	.273	.030	.017	0	11.35	10.63	1.53	—	—
	U117ST	2.60	12.25	23.	1.228	1.49	1.25	1.50	0	.125	12.7	11.1	2.00
	1062	.018	0	.120	.193	.060	.067	16	6.64	14.35	.85	—	—
20	[illegible]119ST	2.72	12.45	22.	.819	.81	1.00	1.13	.010	.108	31.3	24.5	2.66
	.080	.003	.002	.150	.283	.040	.050	2	—	—	—	—	—
21	[illegible]121[illegible]	2.85	12.75	23.6	.646	.14	.35	1.50	0	.090	40.1	25.3	4.00
	.090	.002	.003	.164	.210	.026	.015	0	—	—	—	—	—
22	[illegible]123[illegible]	2.85	12.75	19.4	1.228	1.49	1.25	.75	0	.090	39.8	24.1	4.00
	.101	.011	.013	.157	.300	.036	[illegible]	0	12.33	[illegible]	1.43	—	—
23	[illegible]125[illegible]	2.60	12.75	23.	1.228	1.49	1.25	.75	0	.090	13.5	12.9	.33
	.0[illegible]	.017	0	.132	.200	.066	[illegible]	[illegible]	11.14	13.13	.43	—	—

← Fm 17 →

GA Form [illegible]

Deck No. 3314.000

TRANSMITTAL FOR DIGITAL COMPUTATION

D.T.B. ______ RETURN TO ______

	Weld No. / M Z_{13}	C Z_1 / M_c Z_{14}	V Z_2 / M_c Z_{15}	T Z_3 / H Z_{16}	Wd Z_4 / P Z_{17}	G_p Z_5 / B Z_{18}	G_c Z_6 / E_p Z_{19}	°F Z_7 / X Z_{20}	ν Z_8 / I_m Z_{21}	D Z_9 / T_t Z_{22}	F_{tu} Z_{10} / A_t Z_{23}	F_{ty} Z_{11}	e Z_{12}
24	U1278T	2.84	12.35	23.5	.710	.14	.75	1.50	.020	1.25	26.0	24.5	3.00
	.055	.005	.001	.144	.270	.036	.087	0	7.98	12.50	.34		
25	U1238T	2.60	12.30	23.5	1.216	.14	1.15	1.50	.020	.090	26.5	23.1	2.33
	.070	.023	0	.135	.218	.066	.050	4	6.48	14.38	.79		
26	U1[illegible]T	2.73	12.5	21.5	.900	.81	1.00	1.13	.010	.108	27.9	24.3	2.33
	.074	.013	.001	.149	.250	.066	.043	1	9.21	10.00	1.08		
27	[illegible]	2.10	12.25	23.5	.652	.14	.75	.75	0	.090	19.2	18.6	2.00
	.051	.010	[illegible]	.114	.180	.040	.084	2	5.62	8.13	.40		
28	[illegible]	2.85	12.70	23.5	[illegible]	1.49	1.25	.75	0	.090	34.6	24.8	3.00
	.077	[illegible]	.003	.139	[illegible]	.033	.038	21	11.44	7.50	1.20		
29	[illegible]	[illegible]	12.30	23.5	1.172	[illegible]	1.25	.75	0	.125	19.1	18.6	2.00
	[illegible]	.020	0	.143	.200	[illegible]	.055	5	5.85	14.38	.69		
30	[illegible]	2.85	12.25	23.5	1.175	.47	.75	1.50	0	.090	40.9	27.1	4.33
	[illegible]	.012	.006	.146	.293	.043	.047	17					
31	[illegible]	2.60	12.25	11.6	.640	.26	.75	1.50	.017	.125	20.4	23.8	1.33
	[illegible]	[illegible]	.005	.153	.270	.033	.029	0					
32	[illegible]	[illegible]	12.25	19.5	1.172	1.49	1.25	.75	.018	.125	35.4	24.4	3.00
	[illegible]	.013	.006	.160	.285	.050		4	8.20	11.25	.91		
33	[illegible]	[illegible]	12.25	19.5	1.172	1.49	.75	1.50	.020	.070	38.3	23.4	4.00
	[illegible]	[illegible]	.009	.167	.293	[illegible]	.030	1	4.70	3.13	.006		
34	[illegible]	[illegible]	[illegible]	23.5	.650	[illegible]	1.25	.75	.020	.090	36.9	25.6	3.00
	.070	[illegible]	[illegible]	.140	.280	[illegible]	.028	8	3.67	1.38	.95		
35	[illegible]	[illegible]	[illegible]	19.5	1.172	[illegible]	.75	.75	.019	.090	35.3	26.7	3.66
	[illegible]	[illegible]	[illegible]	.155	[illegible]	[illegible]	.043	0	8.65	[illegible]	.75		

← omit →

GA Form GD323-1

Deck No. 3314.000

TRANSMITTAL FOR DIGITAL COMPUTATION

D.T.G. ______ RETURN TO ______

	Well No. / M Z_{13}	C Z_1 / Mc Z_{14}	V Z_2 / Ms Z_{15}	I Z_3 / H Z_{16}	Wd Z_4 / P Z_{17}	Gp Z_5 / B Z_{18}	Gf Z_6 / Ep Z_{19}	F Z_7 / X Z_{20}	J Z_8 / Mt Z_{21}	D Z_9 / It Z_{22}	Ftu Z_{10} / At Z_{23}	Fty Z_{11}	e Z_{12}
36	U1378T	2.35	12.75	19.6	.67[illegible]	.26	1.25	.75	.021	.125	39.4	23.8	4.33
	.094	.006	.005	.176	.2[illegible]0	.20	.033	0	11.67	7.50	1.41		
19	U1408T	2.60	12.25	23.5	.[illegible]	1.49	1.25	1.50	.020	.125	16.6	15.6	2.00
	.055	.005	0	.130	.2[illegible]	.040	.058	2	11.75	6.58	.87		

A Form 303

WELDING UNIT NO. 2

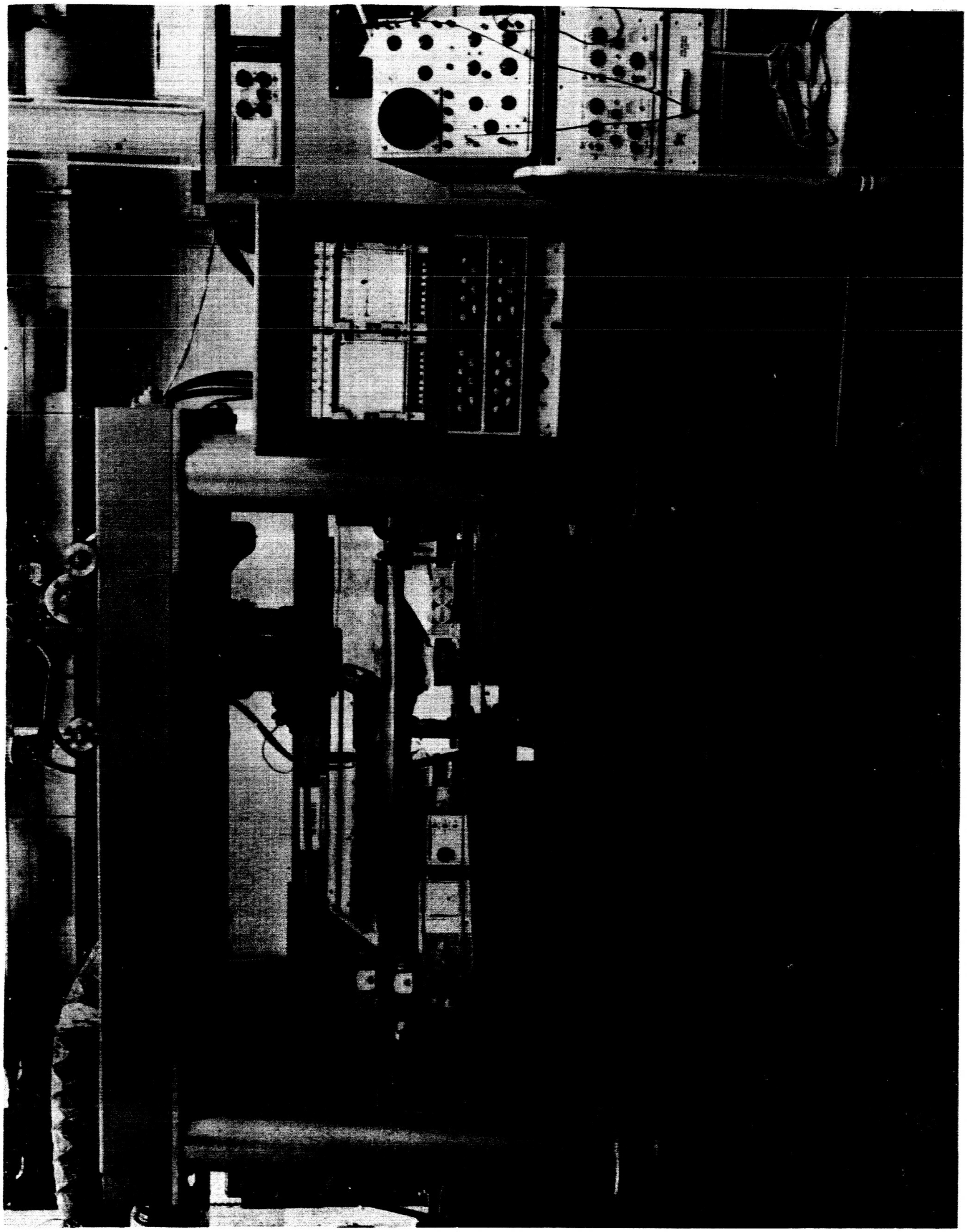

WELDING UNIT NO. 1

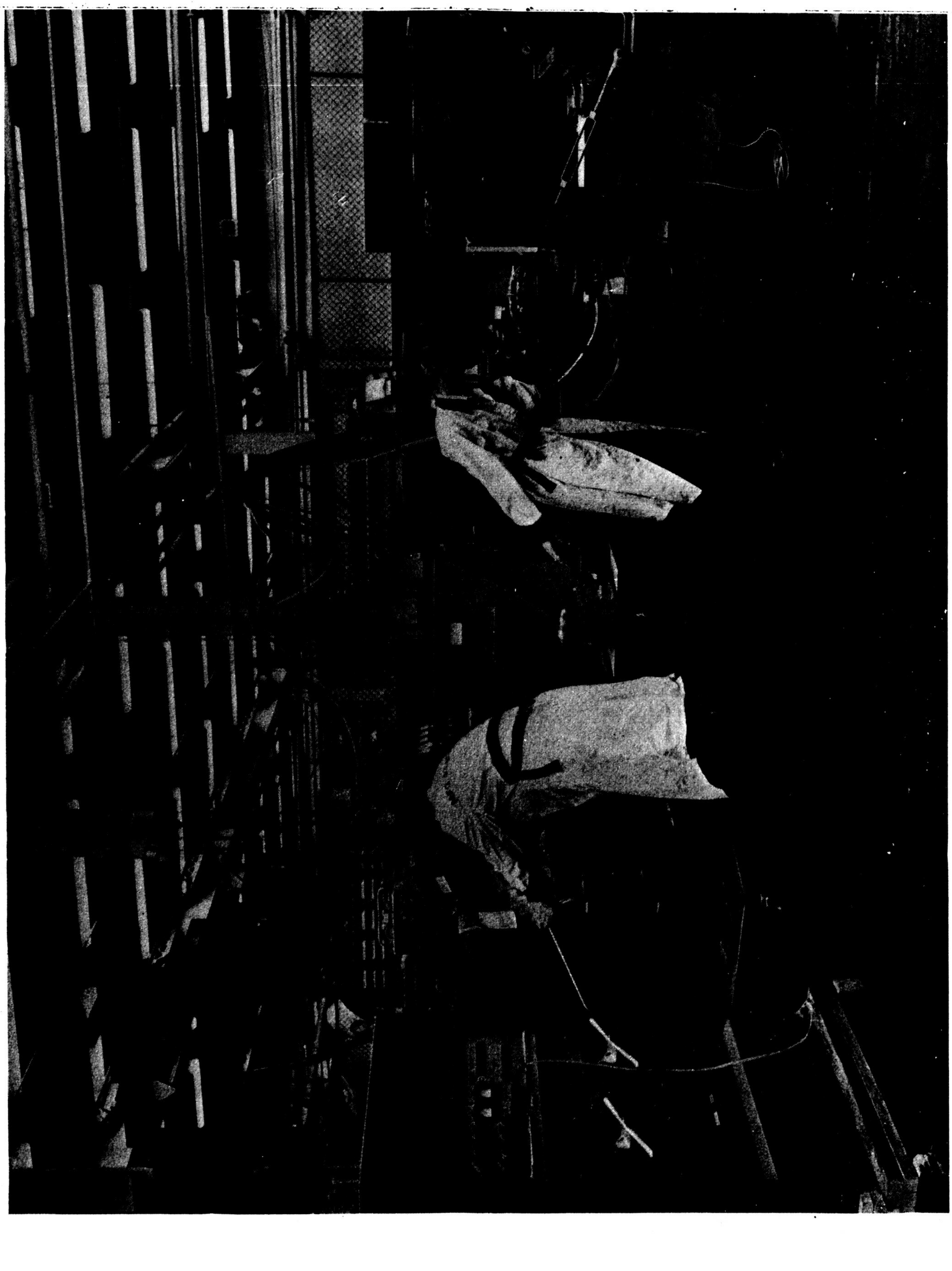

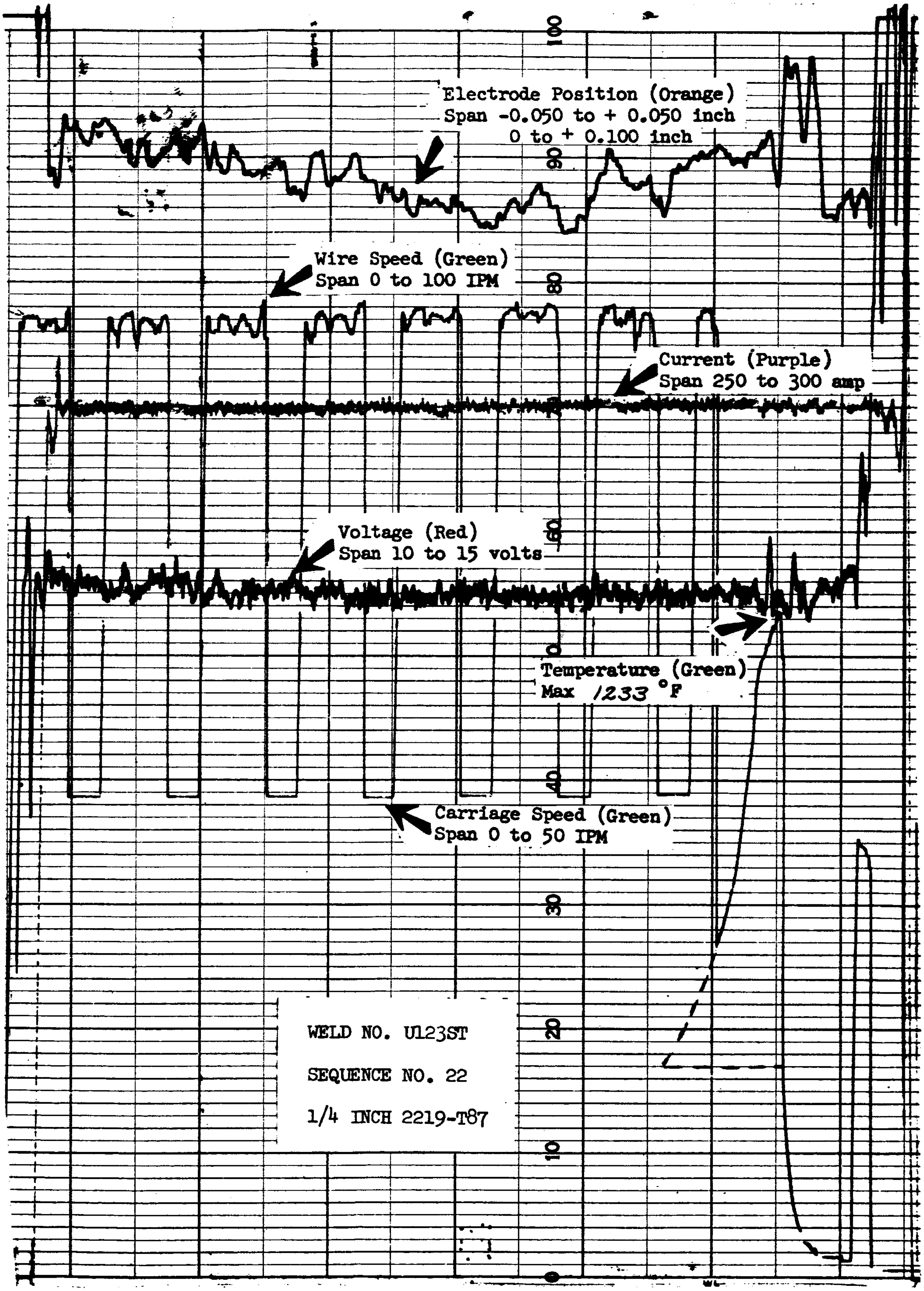
Electrode Position (Orange)
Span -0.050 to + 0.050 inch
0 to + 0.100 inch
Wire Speed (Green)
Span 0 to 100 IPM
Current (Purple)
Span 250 to 300 amp
Voltage (Red)
Span 10 to 15 volts
Temperature (Green)
Max 1233 °F
Carriage Speed (Green)
Span 0 to 50 IPM
100
90
80
60
40
30
20
10
0
WELD NO. U123ST
SEQUENCE NO. 22
1/4 INCH 2219-T87

ANALYTICAL AND STATISTICAL STUDY ON THE EFFECTS OF POROSITY LEVEL ON WELD JOINT PERFORMANCE

PROGRESS REPORT, 18 FEBRUARY 1965
Presented at Marshall Space Flight Center by John F. Rudy - Martin Denver

I. OBJECTIVE

The objective of this program is to establish a correlation between defects — primarily porosity — and mechanical behavior of a weld. A more specific objective is to be able to use this relationship to derive working weld acceptance criteria. It is recognized that the industry is already in operation with not one, but several weld acceptance criteria. This program does not intend to duplicate these criteria, but to make them more definitive. In essence, the benefit of this program is to place the user in a position to confidently accept more defects in the as-is condition, so that the introduction of the specific defect, which is weld repair, will be minimized. This argument can be more fully appreciated when consideration is given to the reduction in mechanical properties which is caused by multiple repair.

II. DISCUSSION

The practical success of this program depends on the ability to make the criteria more definitive. If relationships for more accurate prediction of the influence of a defect are to be made, the defect must be more accurately defined in terms of those characteristics of the defect which influence the mechanical properties of the joint. Thus, we must develop a classification system which considers, in greater detail than present criteria, size, shape, and position of the defect with respect to the boundaries of the weld puddle. Once the classification system is derived, the relationship between the system and mechanical properties will be established by a straightforward empirical approach using statistical techniques.

The first task in the study of defects is to find the defects to study. The practical task to which the program has been addressed for the larger part of the effort to date, is to find a means of producing defects with sufficient predictability and consistency of occurrence to allow a statistically planned and efficient program to be conducted. If we are to obtain the

II. DISCUSSION (Continued)

required numbers of defects within a given classification, we must develop a technique for producing defects which introduces a minimum of welds which must be scrapped as good.

At the beginning of the program it was established that the defects which would be produced would be done so with a minimum of deviation from standard welding procedures. This is necessary in order that the influence which is measured reflects the defect itself, rather than the means which was used to produce the defect. Since current technical thinking attributes the larger part of porosity type defects to hydrogen or water vapor, artificial means of introducing these contaminants have been the primary experimental variables.

III. PRESENT STATUS

Contaminants have been introduced to weld beads by contaminating the surface of the weld filler wire, or by contaminating the shield gas which surrounds the electrode. Filler wire treatments have included the following:

1. As received.
2. $600^{\circ}F$ dry atmosphere bake.
3. Surface cleaning with an alkaline solution.
4. Exposure of the wire to high-humidity, warm air.
5. Soak wire in hot water.
6. Anodize the wire with various current densities, bath temperatures, and times to obtain a porous coating.
7. Cathodically charge wire with hydrogen.

The above wire treatments generally did not give sufficient porosity, in the downhand welding position, to enable a broad range defect study. The anodized wires did give porosity, but not enough to provide the whole range of experimental interest. Perhaps later work on horizontal position welding will show more promise for these techniques.

The second technique, adding contaminant gas to the shield gas, has been more successful in providing a controlled and predictable level of porosity. We have added moisture up to a dew point of approximately $+40^{\circ}F$, and hydrogen

III. PRESENT STATUS (Continued)

up to the ratio 15 CFH hydrogen to 80 CFH helium, and have added mixtures of the two gases in levels up to these values. Cross-section micrographs and x-rays were shown which demonstrated that, with flat welding, the high extreme of porosity which is of interest was obtained with a +25°F dew point, zero hydrogen; or with low dew point (as received), and 5/80 hydrogen. In the horizontal welding position "bad" porosity was obtained with lesser amounts of hydrogen and moisture. A conclusion from these data is that predictable levels of porosity can be obtained with horizontal welding at contamination levels which are sufficiently low to have a minimal influence on arc stability and arc heat input. Thus, a modification of the program was suggested which places the major emphasis on horizontal welding, which will be followed by verifications in the defect-porosity characteristic in the vertical and flat positions.

Side effects were illustrated in terms of arc current and arc voltage stability with various levels of contamination. Side effects were also illustrated in terms of bead surface, showing a deterioration in surface smoothness with increasing hydrogen or moisture.

IV. CONCLUSION

The conclusion which can be offered at this time is that the program has developed sufficient background information to enable predictable and controllable introduction of defects to aluminum welds. We had preliminary correlations between mechanical properties and defective welds to establish the range of experimental interest for a controlled statistical program. At this time, we are able to initiate the intentional defect program in a statistical fashion to develop the final correlation which is the objective of the program. Mechanical properties will be reported in both longitudinal and transverse tension, ultimate strength, tensile strength, bead shape, welding parameters, and elongation in gage lengths of .2, .4, .6, .8, 1.0, and 2.0 inches.

LIST OF ATTENDANTS
(As Recorded)

R. Hoppes	NASA
D. Poorman	NASA
G. Parks	NASA
Ned O. Kraft	Alcoa
W. E. King	Alcoa
G. O. Hoglund	Alcoa
R. W. Reck	Martin
J. F. Rudy	Martin
G. E. Spangler	Reynolds Metals
Carson L. Brooks	Reynolds Metals
F. D. Seaman	Westinghouse
C. L. Cline	United Tech.
M. W. Brennecke	NASA
E. Boardman	Boeing
M. E. Carroll	NASA
E. B. Stewart	NASA
F. J. Jackson	NASA
D. G. Cole	Harvey Aluminum, R&D
R. E. Monroe	Battelle
D. L. Cheever	Battelle
D. D. Pollock	Douglas
C. Hays	NASA
F. R. Baysinger	Kaiser Aluminum
H. Wuenscher	NASA
W. Kuers	NASA
C. McAllister	NASA